UNIVERSITY OF WASHINGTON

DEPARTMENT OF OCEANOGRAPHY

Seattle 5, Washington

Technical Report No. 57

THE MEASUREMENT OF TRANSPORTS AND CURRENTS IN SMALL TIDAL STREAMS BY AN ELECTROMAGNETIC METHOD

by

Richard M. Morse, Maurice Rattray, Jr.,
Robert G. Paquette, and Clifford A. Barnes

Office of Naval Research
Contract Nonr-477(10)
Project NR 083-012

Reference 58-1
August 1958

RICHARD H. FLEMING
Executive Officer

ABSTRACT

Potentials associated with saline water moving through the earth's magnetic field were measured across tidal streams at Mosquito Pass, Westcott Channel, and Deception Pass, Washington. These channels have comparatively small width-to-depth ratios (25, 10, and 5 respectively), and are narrow, less than 200 yards wide, compared to such bodies as the English Channel and the Gulf Stream where other investigators have previously made successful measurements of potential.

The potentials have been related to water transport but, as in the large channels, there are too many variables to allow calculation of the transport-potential or velocity-potential relationships directly from theory.

Calibration with independent transport or velocity measurements remains a preliminary requirement for practical use of this electromagnetic method. Observed potentials at Westcott Channel were calibrated with transports computed from tidal-prism volumes; potentials at Deception Pass were calibrated with predicted surface-current velocities in that stream. Both methods of calibration provided a means of relating the record of potentials to water motions, and velocities and transports obtained from the electromagnetic observations were in satisfactory agreement with previously known data.

Because of the "shape factor", the variable distributions of velocities and the electrical effects of the channel boundaries become more important in smaller streams than in larger channels, whereas the effect of a conducting channel-bed is less important. The magnitude of

the total potential generated is small in streams of small transport, consequently transient potentials and errors due to concentration cells, thermogalvanic cells, and electrochemical abnormalities of the electrodes cannot be neglected. In addition, the tidal variation of the cross-sectional area of these smaller channels must be considered in transport calculations.

In that satisfactory observations have now been extended to very small streams, the electromagnetic method for measurement of tidal stream velocities and transports is considered proved to a degree sufficient to justify its classification as a practical oceanographic tool.

Some consideration is taken of how transports or potentials may be affected by meteorological factors, by runoff, and by anomalous water-motions in adjacent large channels.

ACKNOWLEDGEMENTS

The authors are indebted to Dr. Richard H. Fleming for his encouragement and constructive suggestions, and to the many members of the staff of the Department of Oceanography who gave generously of their time to help with work in the field and in the laboratory.

Appreciation is expressed to Mr. Chester Ullin and Mrs. Houde, who permitted access to their properties at Westcott Channel and Mosquito Pass. Particular mention must be made of the cooperation of the Washington State Department of Highways; the Washington State Park Commission; and Mr. A. V. Henry, Superintendent of Deception Pass (Cranberry Lake) State Park.

Certain data were provided by the U.S. Coast and Geodetic Survey; U.S. Geological Survey; U.S. Naval Air Station, Whidbey Island; and U.S. Air Force Base, Paine Field.

Mr. Morse undertook this investigation as part of graduate work sponsored by the U.S. Coast Guard, Training and Procurement Division. The research was supported in part by the Office of Naval Research under Contract Nonr-477(10), Project NR 083-012.

CONTENTS

SECTION I

INTRODUCTION

The research described in this report was undertaken by the University of Washington Department of Oceanography during 1956 and 1957. Its objectives were to evaluate the principles and practicability of the electromagnetic measurement of velocities and/or transports in tidal streams in relatively narrow and deep channels. Such channels are common along the Pacific Coast from Washington northward through the Gulf of Alaska. In many of the local situations embayments are fed by multiple channels in which the relative and total transport vary with meteorological, runoff, and tidal conditions. Existing current measurements are probably insufficient to accurately establish water movement and exchange in any of these embayments. Large anomalies in flow can be expected during stormy periods when it is difficult, if not impossible, to obtain continuous current measurements by conventional methods; consequently a reliable and practicable method is needed to provide a better description of local flow and an insight of its relationship to causative factors. Attention was given to the electromagnetic method because it appeared to have many of the desired prerequisites for use in these fjordlike systems.

The basis of the method is the principle of electromagnetic induction as developed by Michael Faraday, who himself suggested the existence of electric potentials related to water motions in tidal streams (Faraday, 1832). Faraday's early attempts to prove his theory were unsuccessful, but later in the 19th century the predicted effect was noted in conjunction

with breaks in submarine telegraph cables and was found to be clearly related to the tide. During the early 1900's, as well as during and immediately following World War II, potentials with moored electrode systems in the estuarine waters of Great Britain were obtained successfully over distances of the order of a few thousand yards. Longuet-Higgins (1949) has provided a summary of experiments of this type made prior to 1956. Since 1949, electromagnetic potentials obtained between fixed electrodes have been measured and related to water motions in several areas, notably: the English Channel, as reported by Longuet-Higgins (1949) and Bowden (1956); Cook Strait, New Zealand, Olsson (1955); Bering Strait, Pickard and Lyon (1949), and Bloom (1956); and the Gulf Stream, Wertheim (1954). Early investigators were concerned only with the verification of the effect, whereas more recent efforts have been directed almost exclusively to determination of the transports.

Theoretical applications of Faraday's principle have been developed for both ocean and tidal streams by several authors; however, the greater amount of fundamental theory for tidal streams has been presented by Longuet-Higgins (1949) and Longuet-Higgins et al. (1954). Because of the mathematical complexity of the problem of determining transport many assumptions must be made A common assumption is that the channel is very much wider than it is deep, from which a number of other approximations can be made. In general velocities and transports cannot be calculated on a theoretical basis directly from measured potentials. It does, however, provide the justification for a relation between measured potentials and transport, permitting a calibration of the electromagnetic method.

The mathematical developments of Longuet-Higgins (1949) and Longuet-Higgins et al. (1954) were investigated recently for a tidal-stream channel which was but slightly wider than deep (Morse, 1957). Frequently the relative importance of such factors as the effect of a variable velocity distribution and the effect of a conducting channel-bed were reversed, and also certain assumptions previously made in the theoretical application of the electromagnetic principles were found to be open to question. Induced potentials can be calculated only approximately from measured velocities and transports, however for particular situations empirical relationships can be determined by direct measurement of potential associated with the flow.

Sections 2 and 3 describe the observations and conditions at the locations covered by this investigation, and give pertinent calculations. Some notes of oceanographic interest, given in Section 4, show how observed potentials may be related to the effects of such influences as meteorological factors, runoff, and anomalous water motions in larger, adjacent channels or systems. The over-all results of the project, and the conclusions developed therefrom, are summarized in Section 5.

SECTION 2

MOSQUITO PASS - WESTCOTT BAY

2.1 Location and Description

Mosquito Pass is a narrow, relatively deep channel separating San Juan Island from Henry Island in the San Juan Archipelago (Figs. 1 and 2). Figure 3 is a descriptive chart of the central portion of the pass area and locates the positions of three longitudinal sections and a transverse section (ZZ') at the line of electrodes. The section profiles are shown in Figure 4. Pole Island, located near midstream in the narrowest part of the pass, is a large rock having a maximum elevation of about 8 feet above high water. The main channel is to the eastward of Pole Island; the smaller westward channel is very shallow, and at extreme low water consists mainly of tide pools. The shores are predominantly steep and rocky, and kelp beds are prevalent. The few lowlands and bays along the pass generally have narrow gravel beaches, with the shores of the pass and the surrounding highlands exhibiting large quantities of exposed rock and being heavily wooded wherever the slope has permitted a sufficient accumulation of topsoil. The rocks are predominantly argillites and limestones, with many granitic boulders along the glaciated lowlands. Limestone is quarried at nearby Roche Harbor. The complete descriptive geology of the area is given by McLellan (1927). Currents in Mosquito Pass attain velocities in excess of 2 knots, sweeping practically all loose materials from the rocky channel-bed.

Less than one mile north of the southern entrance to Mosquito Pass a channel leads eastward into two bays. This is the common and only entrance

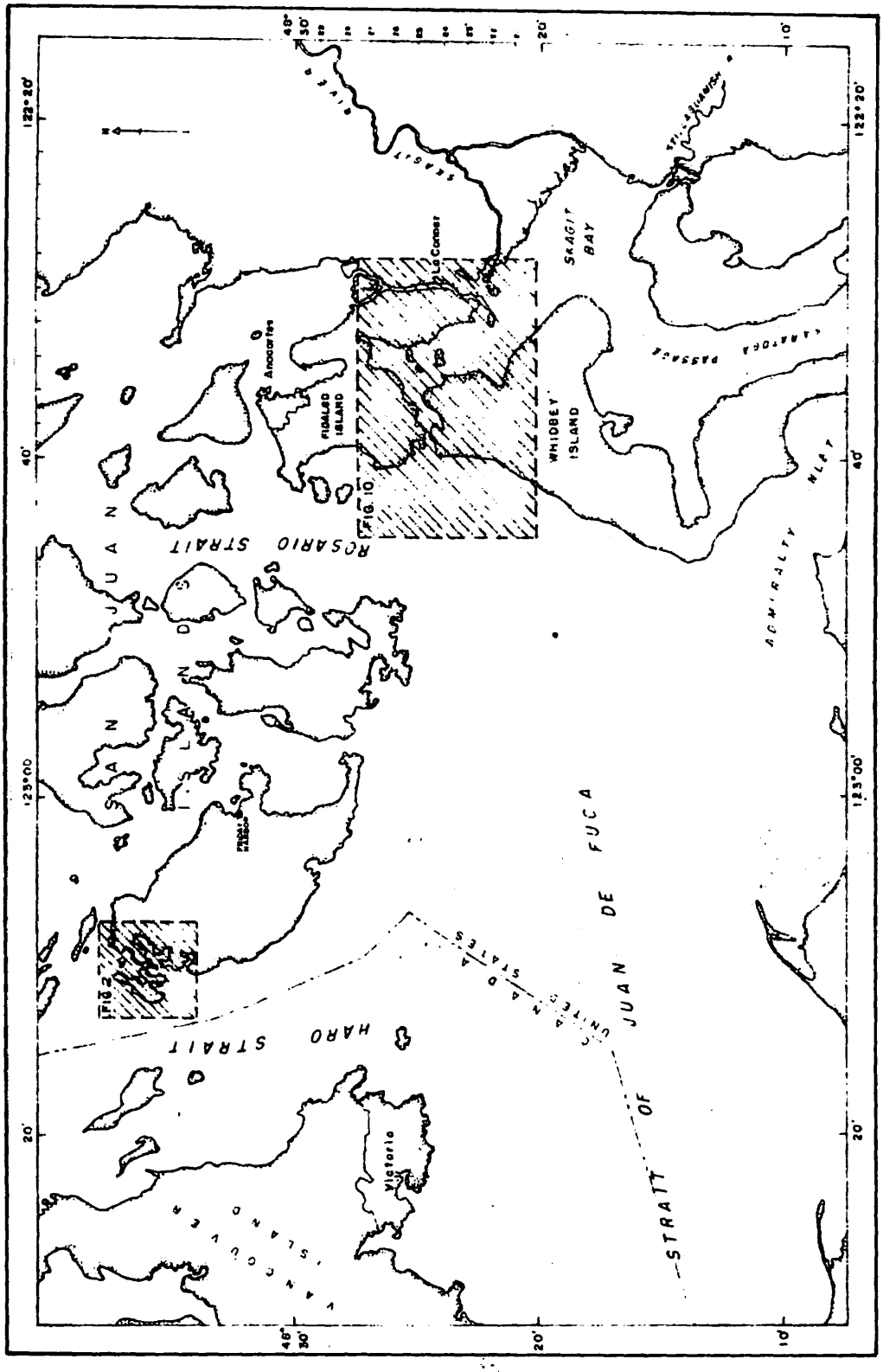

Figure 1. Location of project areas.

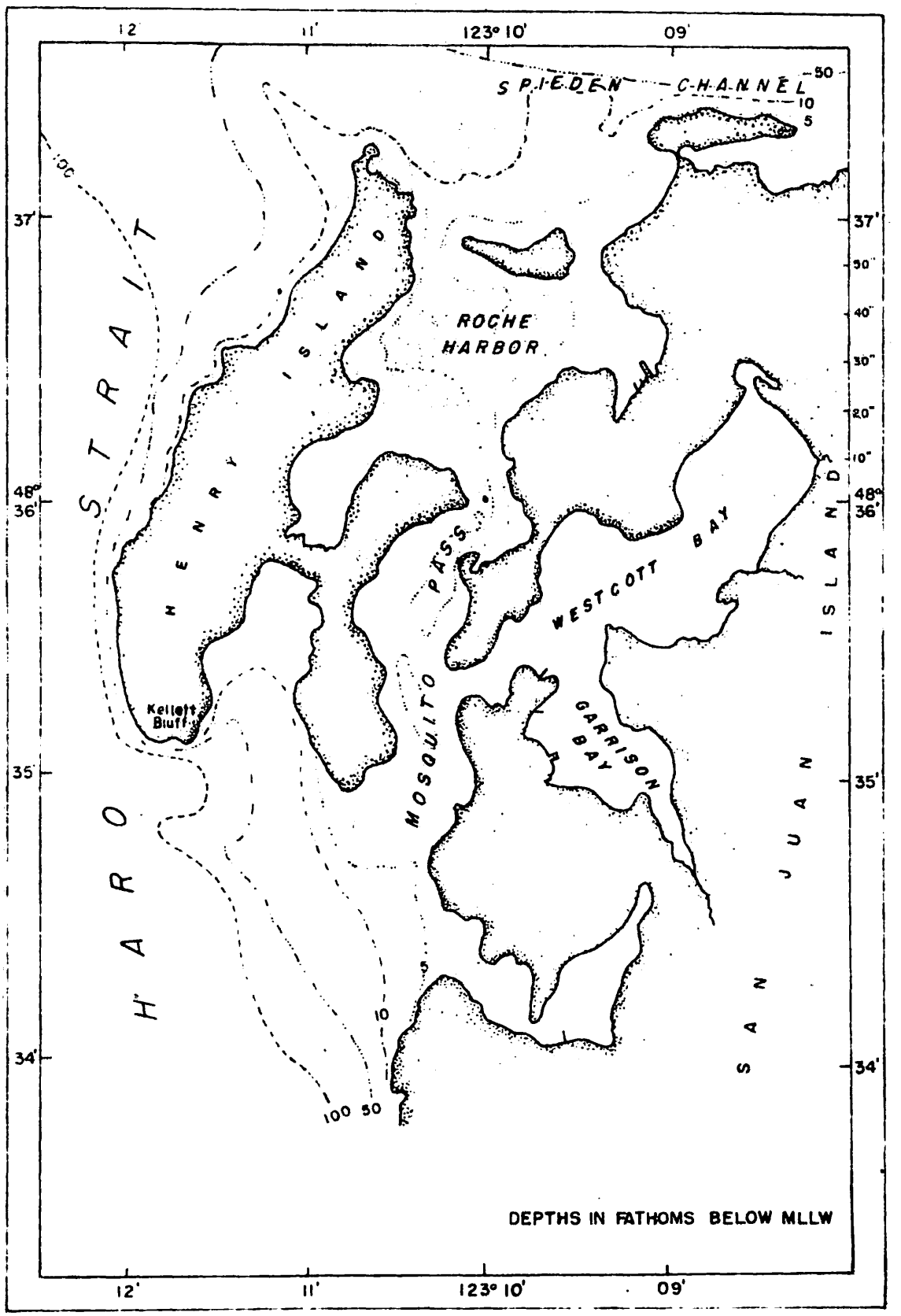

Figure 2. Mosquito Pass and Westcott Bay project area.

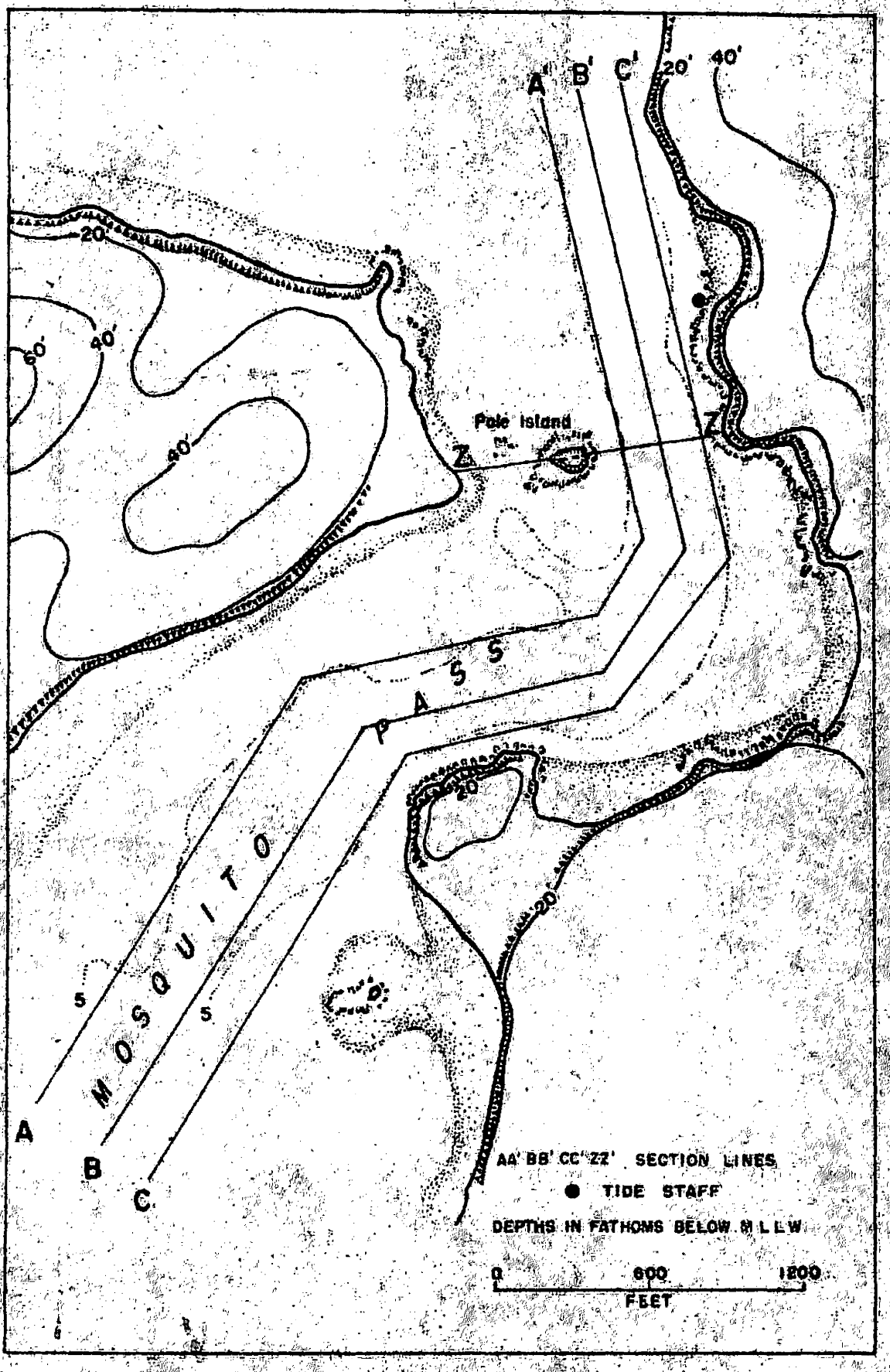

Figure 3. Plan of Mosquito Pass project site.

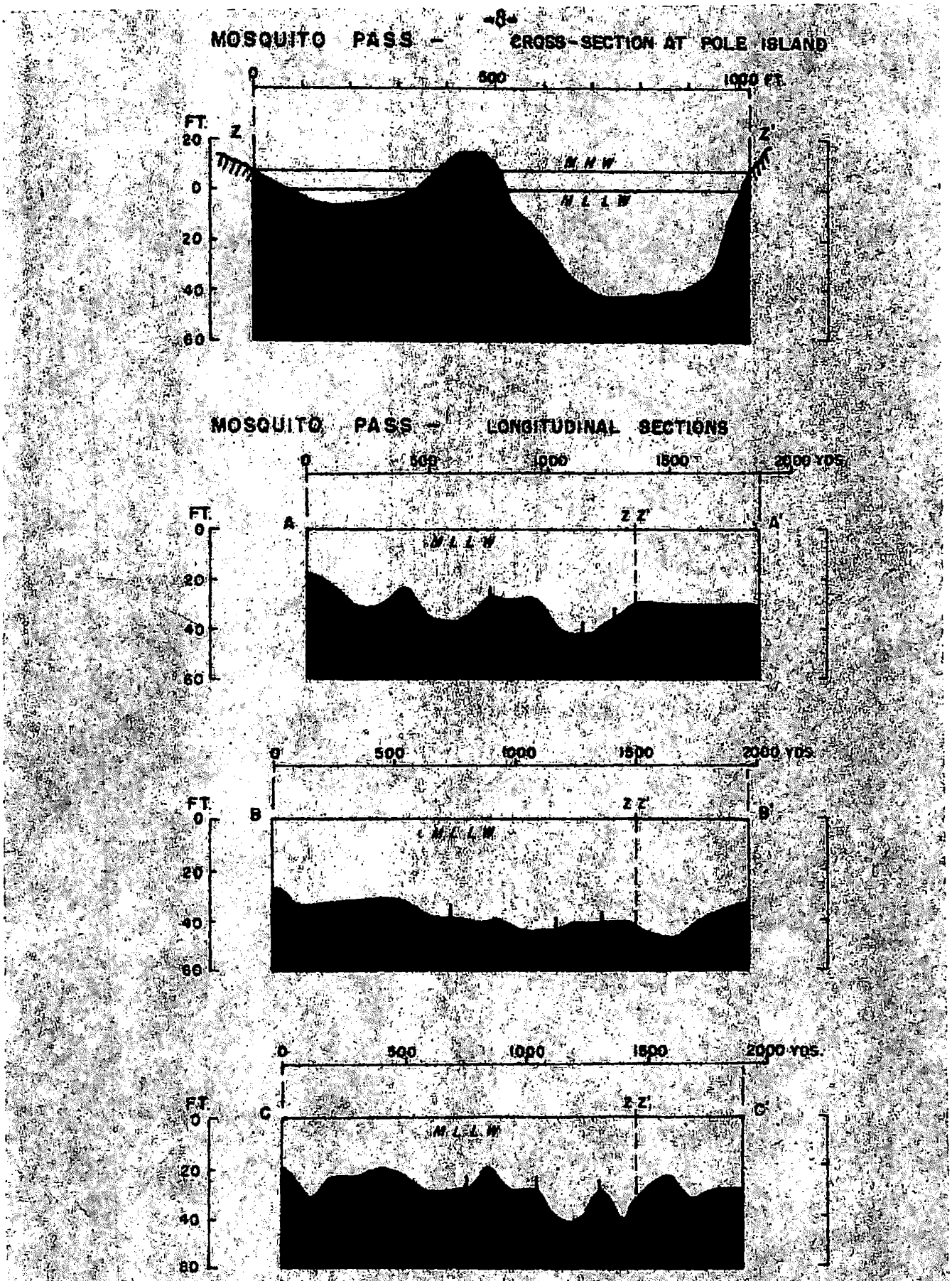

Figure 4. Mosquito Pass sections (vertical pips on bottom profiles show directional changes).

to these bays and will be referred to as Westcott Channel. Westcott Bay leads generally northeast from the entrance channel and is the larger of the two bays; Garrison Bay is a bight southeast of the entrance channel. Both bays are quite shallow, the greatest depth being about 26 feet below MLLW, with the mean depth being much less than this figure. Details of the channel and a transverse section at the line of electrodes are shown in Figure 5. Westcott Channel enters between two rocky headlands, the southernmost rising steeply to over 80 feet. This channel is quite shallow, having a maximum depth of only 21 feet below MLLW. Mean high water is almost 9 feet above MLLW and, at the line of electrodes, the slope of the channel section between the MHW and MLLW lines is nearly vertical. Currents through the channel have about one-half the strength of those of Mosquito Pass and allow a thin layer of silt and fine sand to cover the bottom; otherwise the bottom is only described as "hard" (USC&GS Chart No. 6381).

2.2 Equipment

A recording potentiometer was not readily available at the time of these observations; therefore, a simple measuring circuit unit was constructed from laboratory-type equipment and proved adequate for field work. The unit consisted of a solid wooden box with masonite mounting-panel, into which the following equipment was assembled:

1. Power supply: long-life dry cell, $1\frac{1}{2}$ to $4\frac{1}{2}$ volts
2. A Leeds and Northrup student-type potentiometer with the scale adjusted so as to give a full operating range of 16 millivolts; the smallest marked scale-division on the slidewire was 0.005 millivolt

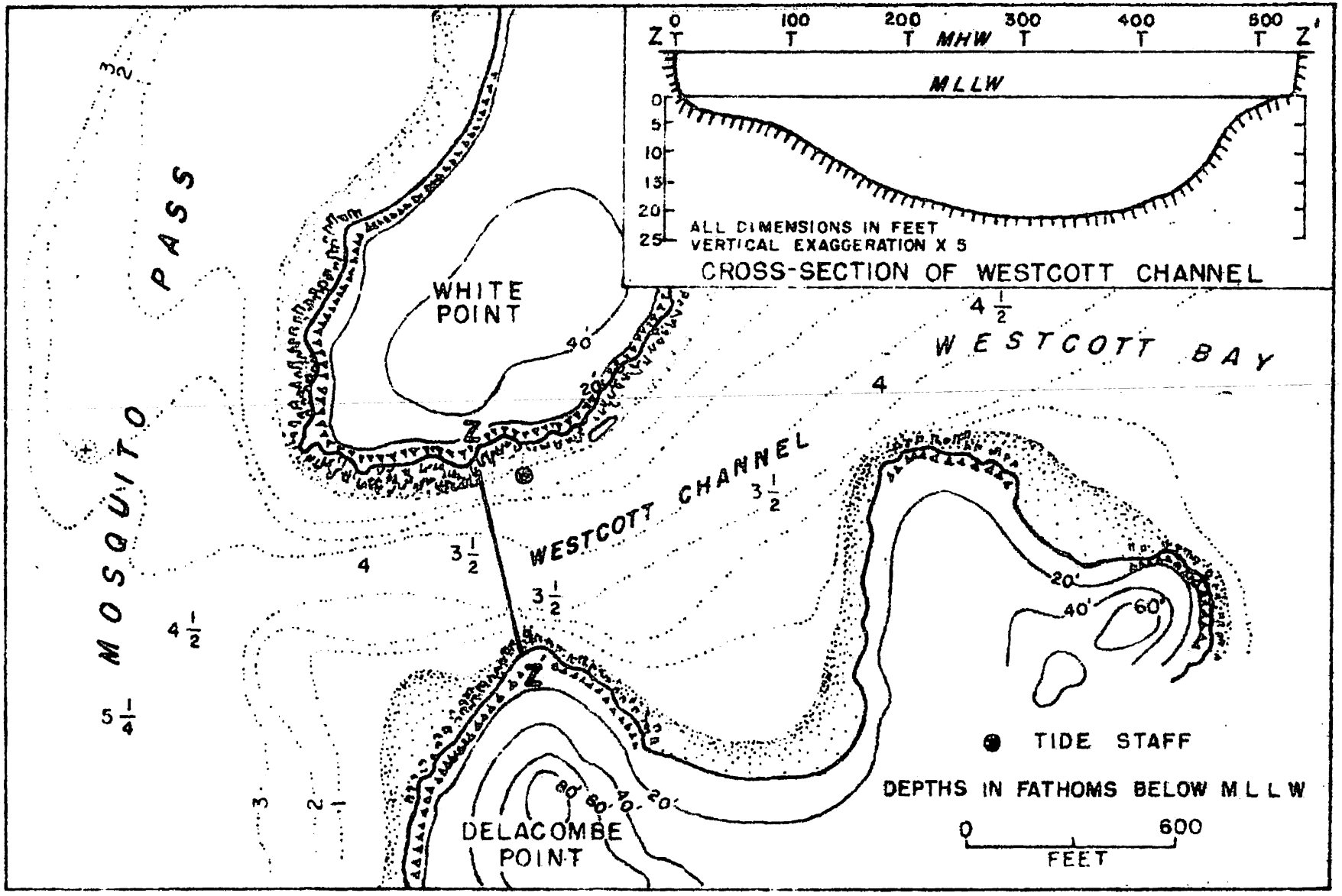

Figure 5. Plan and cross section of Westcott Channel project site.

3. A Weston laboratory-type standard cell, above which was located a switch to shift the circuitry from the standard cell balancing circuit to the input circuit
4. A Leeds and Northrup laboratory-type galvanonometer having a sensitivity of ± 1.5 millivolts, full-scale
5. A polarity switch to adapt the circuitry to changes in the polarity of the potential between the electrodes as the direction of the tidal current changed.

A circuit diagram is shown in Figure 6. Measurements of potential by this unit required manual adjustment of the potentiometer to give zero deflection of the galvanometer needle for each reading. A practiced operator can make measurements at 30-second intervals even during moderately rapid fluctuations of potential, but such a procedure is extremely tedious. Field experiments showed that a plot of readings obtained at 10- or 15-minute intervals would, for the particular conditions found, provide a suitable record. Inspection of an hour's record at each of the three observation locations indicated that reading at 15-minute intervals is generally adequate. Comparative plots of 15-minute readings and 1-minute readings during the same hour are shown in Figure 7. It will be noted that in both Mosquito Pass and Deception Pass a good deal of turbulent detail is lost, and the determination of the time of slack water may possibly lose some accuracy in the 15-minute plot, but these losses do not seem to be serious. In the observations at Westcott Bay, it is difficult to tell the two records apart.

The time schedule of these projects did not allow the fabrication of electrodes especially for this work, so use was made of four silver-silver

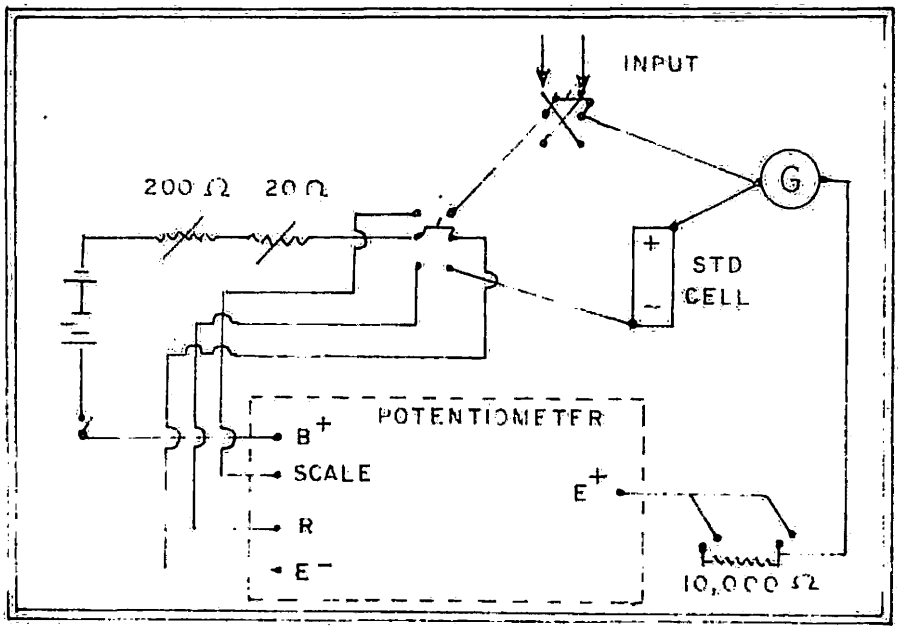

Figure 6

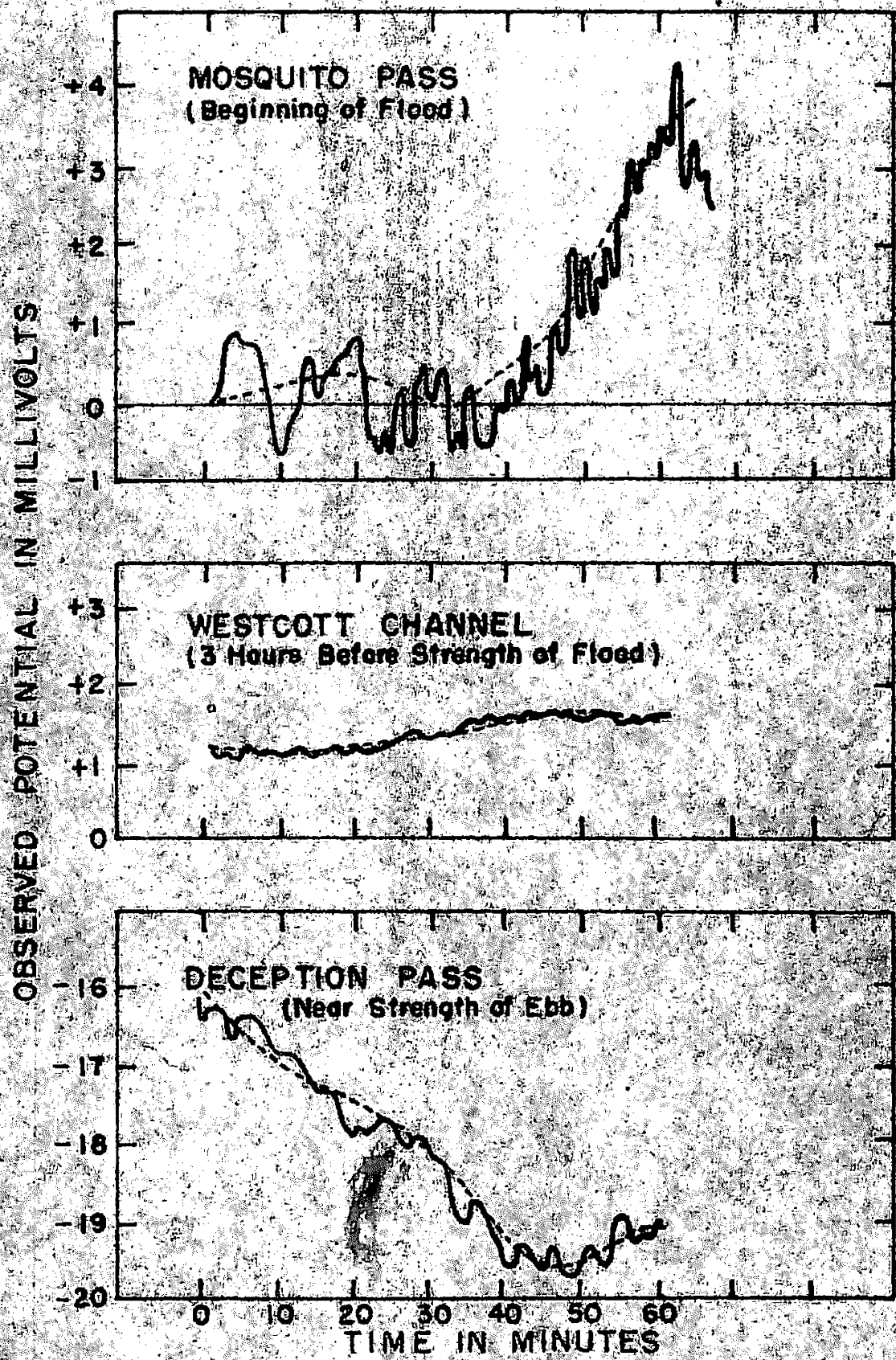

Figure 7. Observed potentials at 1-minute intervals (solid lines) and at 15-minute intervals (dashed lines).

chloride, non-polarizing electrodes which were available from previous GEK studies. These were matched as pairs after observing their individual electrochemical behavior and, by short-circuiting the electrodes together in a container of sea water for a period of several weeks, final residual electrochemical potentials were reduced to less than 0.01 millivolt.

The electrodes finally selected were attached to the connecting cable by unlaying several inches of the stranded wire and by wrapping the wire flatly around the electrode stem, then permanently joining with a low-resistance solder joint. The joint was then wrapped with several layers of self-bonding polyethylene electrical tape under moderate pressure, with particular attention to the end of the connection so that no solder was exposed, and then the entire bond was sealed with Tite-Seal No. 1, a pressure-waterproofing compound.

To protect the electrodes against physical damage during handling in the field, and against being struck by moving objects while positioned in exposed locations, they were encased in micarta (laminated phenolic) housings. These housings consisted of cylinders of paper-based micarta, approximately 9 inches long and 3 inches in diameter, with wall thicknesses of 3/8-inch. Ten holes, $\frac{1}{2}$-inch in diameter, were drilled in each casing to allow ready access of water into the interior. The electrodes were wrapped in several layers of glass wool, which supported each electrode in the center of its housing as well buffering against environmental changes and keeping the electrode surfaces free from contamination. After assembly of the electrode into the housing, the ends of the cylinder were closed with force-fitted linen micarta plugs, $\frac{1}{2}$-inch thick, and the final seal was made in such a

manner that all strain from the weight of the completed electrode assembly was taken by the cable and the housing.

In both areas, the electrodes were positioned by hand a few feet below the MLLW line, being merely laid on the bottom and anchored in place by a covering of small rocks. The cable connecting the electrodes was laid from a small boat at low slack water and was itself anchored every 20 feet by rounded steel weights of approximately 5 pounds each, attached to the cable by marline. In Mosquito Pass the electrodes were placed to avoid large beds of the common kelp Nereocystis, but heavy growths of the large flat-leafed algae (Iridea, Alaria, Laminaria, and Cymathere) in the area prevented the cable from resting directly on the bottom. A diver reported that the cable was often suspended point-to-point, thus allowing it to swing with the current or with the waving of the kelp. Such a situation was highly undesirable and probably accounts for much of the recorded "turbulence"; however, the study in this area was a test of equipment and procedure only and did not justify the effort required to correct the cable suspension.

In Westcott Channel, the cable rested securely on the bottom since no bulb kelp was present and the flat kelps were less troublesome than in the pass. During the last week of observation the electrodes were buried about 12 inches deep in the gravelly sand of the shelves that extend out immediately below the MLLW line on either side of the channel. No change was noted in potential, nor in the character of its fluctuation. No doubt some stabilization of the electrode environment accompanied this relocation, but the effect was not apparent on the record.

The electrode lines were established as nearly normal to the predominant current directions as possible and the measuring unit was located

to give the observer an unobstructed view of the channel for the purpose of noting surface-flow patterns. Tide staffs were located in somewhat sheltered positions near each electrode line. Tide heights were measured visually at 15- to 30-minute intervals and were found to compare favorably with the predicted tide heights for Roche Harbor, although certain anomalies were noted in Westcott Channel. Most common of these anomalies was the daily predicted HHW being generally observed as the lower of the two daily high tides; however, such phenomena are not unusual in the entrances of closed basins. The primary purpose of the tide staff in this instance was to provide the basis for calculating tidal-prism volumes to be used in the attempted calibration of the electromagnetic method.

2.3 Tidal Currents and Velocity Distribution

Since the tides in this area are a mixture of the standing-wave and progressive-wave types, the tidal current showed no obvious relation to the stage of the tide. Slack current did not coincide with the times of high or low water, and the time of strength of current was not the same as the time of midtide. The duration of the ebb in nearby Haro Strait is longer than that of the flood, and this time-relation is often magnified in Mosquito Pass by hydraulic effects; in Mosquito Pass ebb currents associated with large changes in tidal height have been observed to extend over a period of 10 hours. Here, observed potentials indicate that within an hour of surface slack the surface-current direction gives a poor indication of the direction of the net transport of the stream. At least two layers of flow are present at these times, and measured potentials indicated a net

flow diametrically opposed to the surface flow. The existence of this reverse current was noted several times while water samples were being taken at depth and was confirmed by a diver during an examination of the cable.

Perhaps the most interesting feature in Westcott Channel is the horizontal distribution of the tidal currents. Part of the northward-flowing flood current in Mosquito Pass is sharply deflected towards the east by a submerged ridge extending into Mosquito Pass from the north side of Westcott Channel. This feature, combined with the bathymetry of the channel itself, directs the strength of the flood current along the northern side of the channel. The reverse is true, although to a lesser extent, on the ebb. It might be said that only half of the channel is in actual use at any particular time. Observations of floating objects on windless days have shown that on the flood the southernmost one-third to one-half of the channel remains virtually slack or tends to show wide countercurrents of low velocity. During the ebb a narrower band of somewhat stronger countercurrents is observed close along the north shore.

Only a little is known about the local vertical velocity distribution. Several time-studies of short duration in Westcott Channel (Helle, 1955) showed that the maximum midchannel velocity, particularly on the flood cycle, was to be found in the layer 2 to 4 meters below the surface. At strength of current, Helle's observations showed that at a depth of 7 meters (just off the bottom) the velocity averaged approximately one-half of the maximum. Currents in Westcott Channel are somewhat out of phase with those in Mosquito Pass. Maximum velocities through the Channel were

estimated at 1.5 knots during this study; during a period of moderate tidal range, Helle (1955) measured maximum midchannel currents of 1.15 knots.

2.4 Distribution of Temperature and Salinity

The physical and chemical characteristics of the water flowing out of Westcott Channel reflect the local influence of the bay system behind the channel. This is particularly true with regard to temperature. The surface area of this bay system is almost one square nautical mile, allowing a considerable amount of surface heating to the shallow water of the bays. Large mudflats are exposed at low tide at the heads of both bays and in many places along the sides. When the flood occurs during warm daylight hours heat is added to the water from the bottom as well as the top. With this "built-in" heating system, the afternoon ebb discharges, through the entrance channel, water which is as much as 3° C. warmer than the influx. Field studies made during 1955 by the Friday Harbor Laboratories showed that on a typical summer day the surface temperatures at the head of Westcott Bay were as much as 4° C. higher than those at the entrance channel. Waters in the small, shallow estuary at the southern end of Garrison Bay were commonly 10° C. warmer than those of the entrance channel. Measurements made in conjunction with the electromagnetic study showed that the water on the south side of the channel was warmer than that on the north side, regardless of the stage of the tide. The flow patterns in the channel, combined with the existence of the shallow shelf off the southwestern entrance to the channel, are considered partially responsible for this. During summer virtually no fresh water is added to the embayment and, while evaporation

rates are probably quite high, the exchange of water is such that no detectable changes in salinity due to evaporation would occur. A summary of the measured distribution of temperature and salinity in Westcott Channel is shown in Table 1.

Table 1. Temperature and salinity in Westcott Channel

	Flood Cycle								Ebb Cycle	
	July 7		July 8		July 21		August 4		July 8	
Station and Depth	T °C	S °/oo	T °C	S °/oo	T °C	S °/oo	T °C	S °/oo	T °C	S °/oo
Delacombe Pt.										
1 meter	10.7	30.27	10.1	30.46	11.9	29.06	11.4	30.01	13.3	29.74
3 meters	10.1	30.37	10.2	30.49	11.4	29.20	11.6	30.03	12.9	29.76
Midchannel										
1 meter	9.9	30.33	9.9	30.43	11.7	29.22	11.4	30.03	12.6	29.77
7 meters	9.8	30.33	9.8	30.43	11.1	29.39	11.2	29.86	11.7	29.92
White Point										
1 meter	9.9	30.37	10.0	30.44	11.3	29.39	11.5	29.96	12.1	29.83
7 meters	9.9	30.38	9.8	30.44	11.3	29.34	11.3	29.95	12.3	29.57

Some progressive heating during the summer is reflected in the temperatures and, although only the observations of 8 July covered both cycles, that one day is an excellent example of the differences between the flood and ebb waters. Frequently the T-S data indicates apparent instability in the vicinity of one or both electrodes at this location.

The cross-channel gradients of temperature and salinity raise the question of the effects of thermogalvanic and concentration cells. Von Arx (1950) has given 0.69 mv/°/oo as an average value for the salinity coefficient of potential and 0.59 mv/°C for the temperature coefficient.

The actual salinity coefficient can be calculated for any particular gradient. The temperature coefficient does not lend itself readily to calculation although the principles of thermodynamics and electrochemistry allow calculation of the coefficient by methods involving activity coefficients and specific heats. Levin and Bonilla (1951) have studied the thermogalvanic effect for silver-silver chloride electrodes at temperatures above 25° C. in various electrolytes, and have shown the temperature coefficients of potential to be of the order found by Von Arx. From our data it would appear that the effect of concentration cells is apt to be larger on the ebb than on the flood, but generally both would be small. However, the cell effect which could exist at the change of tide could amount to as much as 1.5 mv. Inspection of the record leads to the belief that cell effects did exist throughout the observation periods and that they became progressively larger as the summer heating produced continually increasing differences in the water of opposing flows. The magnitude of these cell effects is discussed in the following subsection on observations and calculations.

2.5 Observations and Calculations

Figure 8 shows a portion of the record obtained at Westcott Channel, plotted without correction. The first anomaly apparent is the periodicity of the fluctuations of potential. These variations appeared continually throughout the five separate days of observation and have a relatively constant period between 45 and 60 minutes. While no explicit explanation for these fluctuations is offered in this report, several possibilities exist:

1. Although the line of electrodes is parallel to the flow in Mosquito Pass it is not parallel to the line of flow in nearby Haro and Juan de Fuca

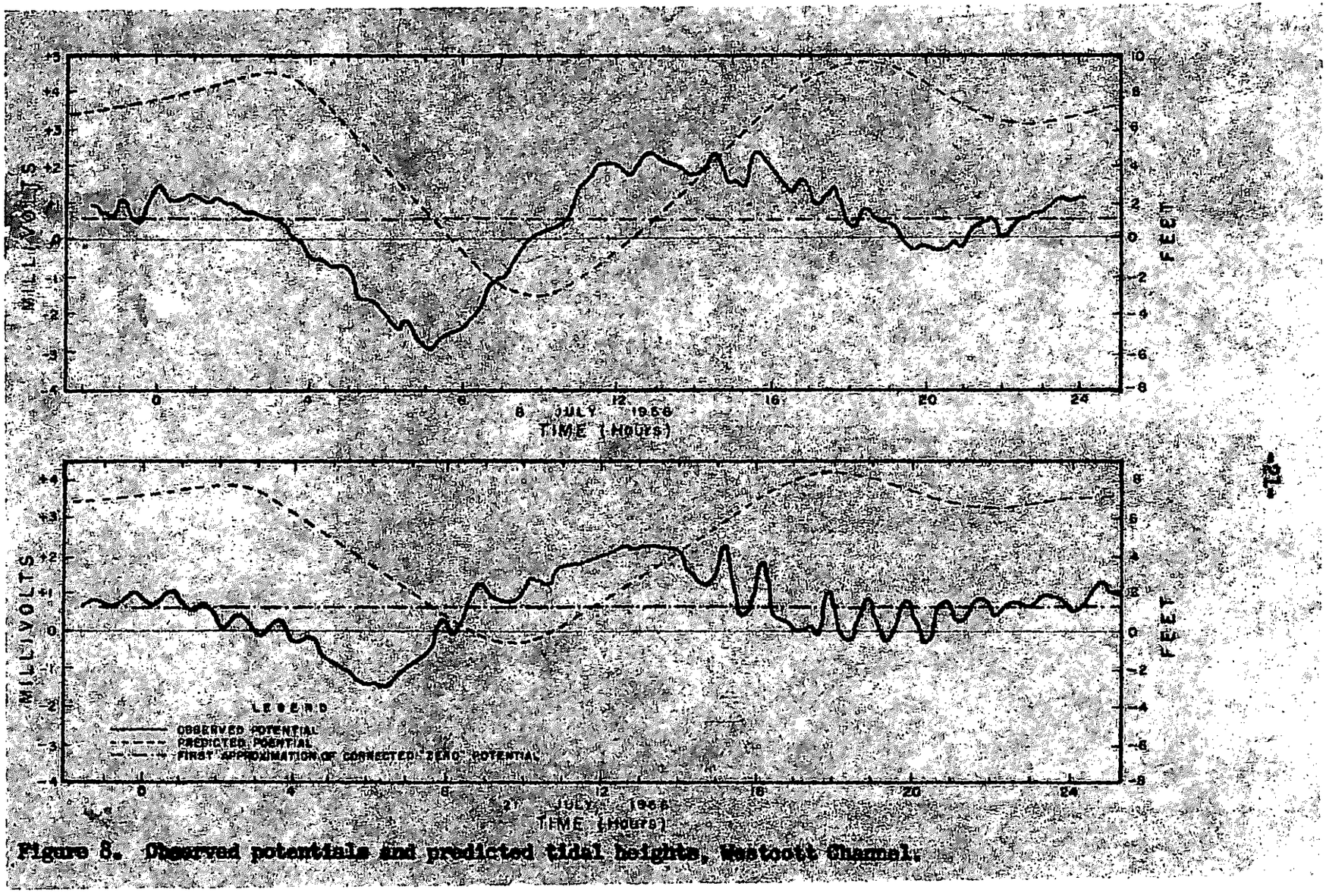

Figure 8. Observed potentials and predicted tidal heights, Westcott Channel.

Straits. Induced potentials of the magnitude and period of the variations found in Westcott Channel possibly may be associated with the water motions of these larger systems. Direct measurements in Haro Strait (Barnes et al., 1956) have shown marked variations in current velocities similar to those reported here in Mosquito Pass.

2. Transverse seiches in the Haro Strait-Juan de Fuca Strait system may cause fluctuations of the water level at the entrance of Westcott Bay. Application of Merian's formula to this Strait system yields an approximate seiche period of 40 minutes, which is in general agreement with the period of variation of potential. The fluctuations of potential are approximately $\pm$ 1 mv at their largest, and later calculations will show that a potential of 1 mv is equivalent to an approximate transport of 150 m^3/sec through Westcott Channel, or equivalent to a mean velocity of 0.15 m/sec. This velocity or transport could possibly be produced by seiches in the straits, of sufficient amplitude to provide a differential hydraulic head of 0.1 cm through Westcott Channel. Calculations show that seiches associated with the Westcott-Garrison Bay system and Mosquito Pass have periods of only a few minutes, and could not be related to the fluctuations of potential.

The electromagnetic potentials were calibrated against the calculated transport of the stream. The volume of the bay system was computed for 1-foot depth increments over the depth range from MHW to a level several feet below MLLW. Tidal heights observed at the entrance to the bay were used to compute the volume of the tidal prism during any given cycle, and knowing the time required for the cycle to run its course allowed the calculation of a mean transport or, assuming an average cross-sectional area of the

entrance channel, the calculation of a mean velocity. The volume of the prism (total transport) was compared with the integrated potential obtained during the same time-interval, to give a simple calibration factor. This factor is only approximate since the variable distribution of velocity strongly suggests that the factor relating potential to transport would be a time variable; however, the effect of the integration over complete cycles should aid in averaging the calibration.

A displaced zero on the record of potentials was apparent in the first transport-potential calculation. Since no checks had been made of the behavior of the electrodes in the field nor had the possibility of cell potentials been investigated while the observations were being made, the zero displacement was computed from transport considerations. It was considered that the net transport, and thus the net potential, must be zero between any times for which the same tidal height was recorded. To eliminate any variations which might exist in the cyclic flow-structure, the transport-potential calculations were made between times of identical tidal height which occurred on the same parts of the tidal cycle--two points separated by a full tidal day. As a first approximation, the zero potential was taken from the record at the times of slack water. Based upon this assumed zero, the positive and negative potentials were then integrated, added algebraically, and compared to zero. If necessary, a second approximation was made. This method gave generally satisfactory results except during the period of daylight hours of 22 July, where it was apparent that the sign of the zero-error had reversed abruptly. This reversal, coupled with the progressive nature of the error, strongly suggests that the error was due to concentration

or thermogalvanic cell effects. The final approximations of the zero-error were:

+0.45 millivolt	7-8	July 1956
+0.61 millivolt	20-21	July 1956
+1.10 millivolt	4-5	August 1956

Errors of the magnitude mentioned above are important in small-scale work. In similar electromagnetic experiments in larger tidal streams a displaced zero of 1 mv would go virtually undetected, since average potentials are measured in 100's of millivolts.

At the end of the operation in Westcott Channel, a field check of the electrochemical zero of the electrode pair showed a startling potential of +11.6 mv. In about 15 minutes this potential had decayed to +3.4 mv and, by the time the electrodes (continuously submerged in a container of water taken from Westcott Channel) had been returned to the Friday Harbor Laboratories, the electrochemical potential was found to be only +0.3 mv. Subsequent checks showed no electrochemical potentials greater than $\pm$ 0.1 mv, and no explanation has been found for the abnormal behavior of the electrodes. Certainly the 11 mv error was not present during the observation period, and in the course of later observations at Deception Pass with the same electrode-pair no electrochemical errors greater than $\pm$ 0.3 mv were noted prior to the time that one of the electrodes was damaged.

The transport-potential calibration factor derived from the computations discussed previously was by no means constant. Average or mean values for areas, volumes, transports, potentials, and cross sections were used throughout; the time-variation of the cell potentials and the cross section

of the channel was not considered except by such averaging. However, the results are not unreasonable, are all of the same order of magnitude, and are consistent with the few direct measurements available. The results of the "calibrations" are given in Table 2.

The estimated value of the maximum midchannel surface currents is in very good agreement with the velocities reported in Section 2.3 from direct measurements. Assuming the transverse section of Westcott Channel to be an ellipse with major and minor semi-axes a and b, respectively, and assuming the tidal stream of Westcott Channel to move with a uniform velocity, then

with: $a = 80.9$ m, $\rho_1 = 30$ ohm-cm, $H_z = 0.536$ gauss

$b = 7.6$ m, $\rho_2 = 10^4$ ohm-cm, $V = 1.0$ knot

$$\frac{\phi}{V} = \frac{2H_z a}{1 + \rho_1 a/\rho_2 b} \times 10^{-8} = 4.20 \text{ mv/kt},$$

and

$$\frac{\phi}{VL} = 26 \text{ mv/kt/km}, \text{ where } L = 2a \text{ (Longuet-Higgins et al., 1954).}$$

The average calibration from transport considerations (Table 2) is approximately 60 per cent of the theoretical calibration.

A plot of the potentials observed at Mosquito Pass is shown in Figure 9. An enlarged section of this plot, showing the rapid fluctuations of potential, was shown previously in Figure 7. Despite the potentials which may have been due to cable movement and transient cell effects, the record indicates that there are large-scale fluctuations of water velocity in the pass. Explanations for this phenomena include: (a) true turbulence due to high velocities through the narrow, irregular channel; and (b), surges of large

Table 2. Summary of transport-potential calculations in Westcott Channel

Cycle	Tidal range	Mean transport $\bar{T}$, m^3/sec	Mean potential $\bar{\phi}$, mv	T/ϕ m^3/sec/mv	$\bar{V}$ kts	ϕ/V mv/kt	Est. Max. V_s* kts	Calibration mv/km/kt
Flood	-0' 2" to 9' 2"	242	1.53	156	0.57	2.68	1.26	16.6
Ebb	9' 4" to -1' 0"	253	1.73	147	0.60	2.87	1.62	17.7
Flood	-1' 0" to 8' 0"	189	0.94	201	0.47	2.01	1.00	12.4
Ebb	8' 5" to -1' 0"	277	1.62	171	0.67	2.40	1.78	14.9

* Velocity at the surface at midchannel is arbitrarily assumed to be 4/3 of the instantaneous mean-velocity.

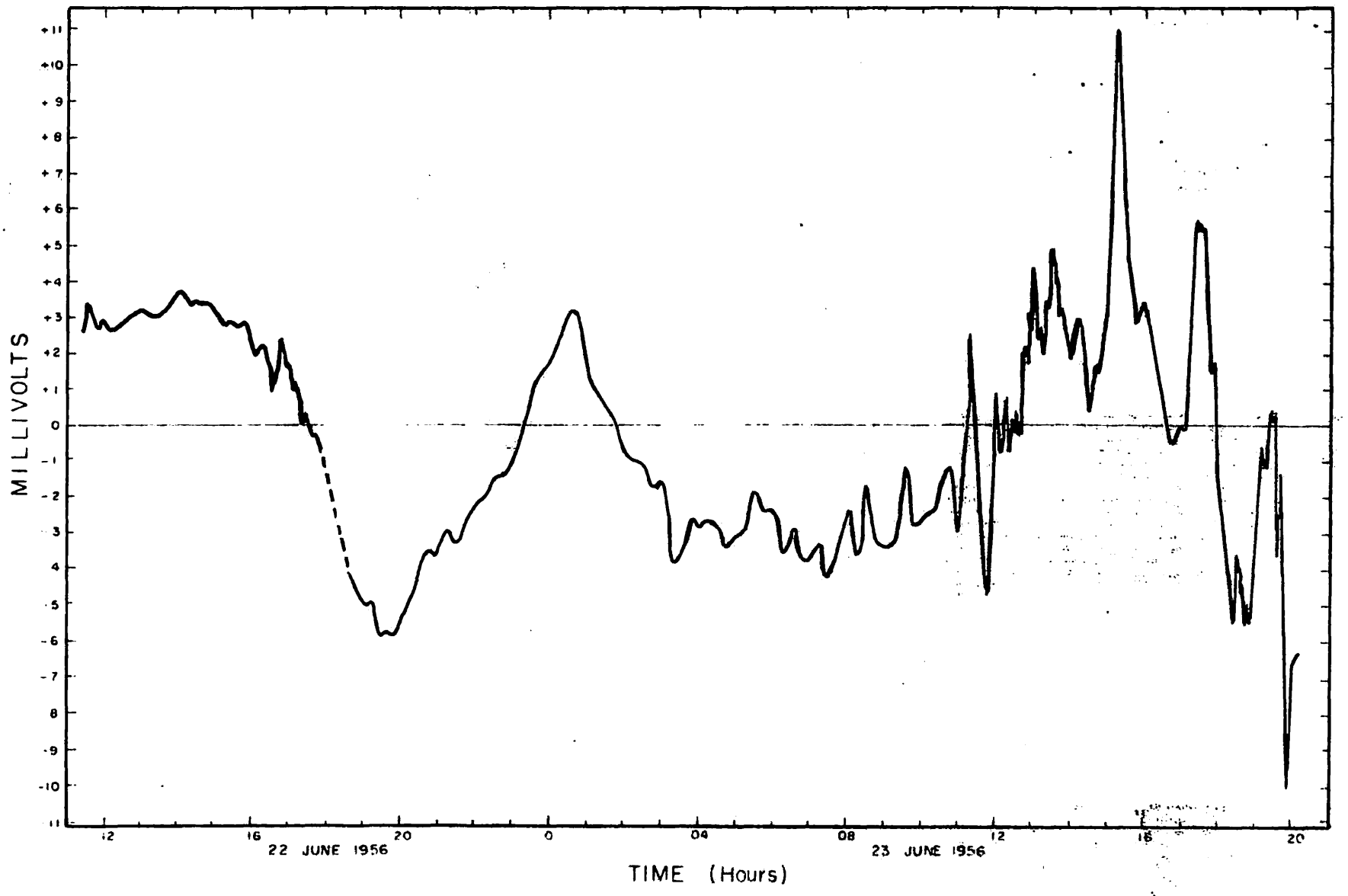

Figure 9. Observed potentials, Mosquito Pass.

parcels of water into the pass from Haro Strait, a large and very deep channel with maximum currents ranging from 2 to 6 knots. The large fluctuation of potential which occurred between 1500 and 1530 on 23 June (Figure 9) was quite real and may be related to the current in Haro Strait, which at that time was at maximum flood of 3.8 knots.

Although the negative surge of potential which occurred later the same day appears to be similar to the positive surge, its source is different. Throughout the experiment efforts were unsuccessful to detect the passage of numerous small boats as they crossed the electrode line. However, at about 1945 on 23 June a large vessel, heavily laden with limestone ore from Roche Harbor, began its southward run down the pass. A nearly continuous recording of potential was made as the ship passed, and the passage of the ship is reflected in the negative surge of potential shown in Figure 9. The rapid increase in potential began while the vessel was still several hundred feet north of the electrode line and the potential, although falling rapidly, was still far above normal for at least 10 minutes after the ship had passed. Pickard and Lyon (1949), in a test operation, observed marked fluctuations of potential as large ships passed close to a moored electrode and they attributed this fluctuation to the change in salinity in the vicinity of the electrode, caused by the propeller action of the ship. Although changes in salinity may contribute to the fluctuations in the instance of the ore boat, the time sequence suggests that this deep-draft vessel was literally pushing a large parcel of water ahead of it and pulling even more water behind. The passage of the ore boat may have resulted also in some transient changes in the local magnetic or electrical field, but this is doubtful

because of the nonmagnetic character of the kilned limestone and the wooden structure of the vessel.

Calculation of the theoretical potentials that might be developed by the flow through the pass shows the horizontal potential gradient to be $\frac{\partial \phi}{\partial x} = 2.76 \times 10^{-7}$ volts/cm/kt. With a channel width of 138 meters between the electrodes, the relation of induced potential to mean velocity would be 3.80 mv/kt. With the further assumption that $\bar{V}/V_{max} = 0.75$, the theoretical calibration becomes 2.85 mv/kt of surface current. These calibrations would indicate that, at the mean strength of current, average velocities in Mosquito Pass are approximately 1.6 knots and surface (maximum) velocities are about 2.1 knots.

Similarities of channel-bed conductivities, water characteristics, and flow patterns in Deception Pass and Mosquito Pass suggest that it is not unreasonable to use the final calibration (Section 3.5.6) for Mosquito Pass. This yields average velocities at strength of current in Mosquito Pass of approximately 1.9 knots, and surface (maximum) velocities of approximately 2.5 knots. The latter figures, based upon an approximate calibration are considered to be in closer agreement with the true situation than are the former figures based upon a theoretical calculation. The 2.5-knot surface velocities estimated by use of the Deception Pass calibration figure compares with the 2.7-knot surface current predicted for Haro Strait at Kellett Bluff on this particular cycle. The only known direct measurement of surface velocities in Mosquito Pass (two observations only, Helle, 1955) indicates maximum velocities in the Pass as being 0.1 to 0.6 knot less than those predicted for Haro Strait off Kellett Bluff.

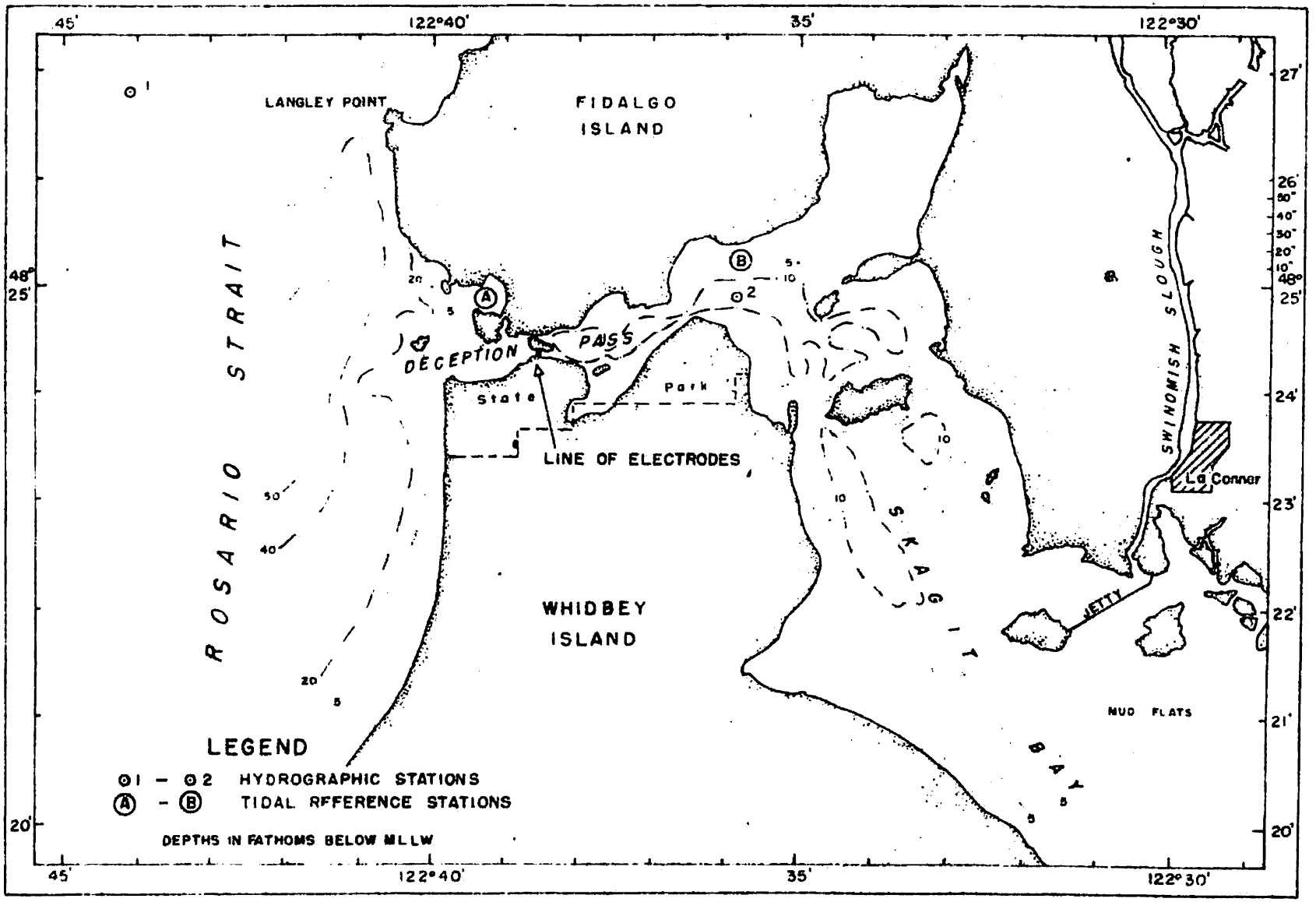

Figure 10. Deception Pass project area.

SECTION 3

DECEPTION PASS

3.1 Location and Description

Deception Pass is a deep, narrow channel separating Whidbey and Fidalgo Islands at the northeastern extreme of Puget Sound. Since Fidalgo Island is separated from the mainland only by a very narrow shallow slough, it may be considered for purposes of gross water exchange that Deception Pass is the only outlet of Puget Sound other than Admiralty Inlet. It should be noted, however, that the average cross-sectional area of Admiralty Inlet is over 100 times as large as that of Deception Pass. Whidbey Island separates the waters of Saratoga Passage and Skagit Bay from those of the Strait of Juan de Fuca and Rosario Strait. Skagit River, the largest river in western Washington, enters Skagit Bay in two forks; one enters near the southern end of the bay where forks of the nearby Stillaguamish River also enter, and the other, the North Fork, enters about midway up the eastern shore of the bay. Figures 1 and 10 show the general location of Deception Pass in respect to surrounding features, and Figure 11 shows the detail of the pass itself. Fidalgo and Whidbey Islands are separated by both Deception Pass and Canoe Pass, these passes in turn being separated only by a small island. Canoe Pass is very narrow and extremely shallow, accounting for less than 10 per cent of the total cross section of the outlet and, due to friction, it probably accounts for considerably less than 10 per cent of the total transport of the outlet.

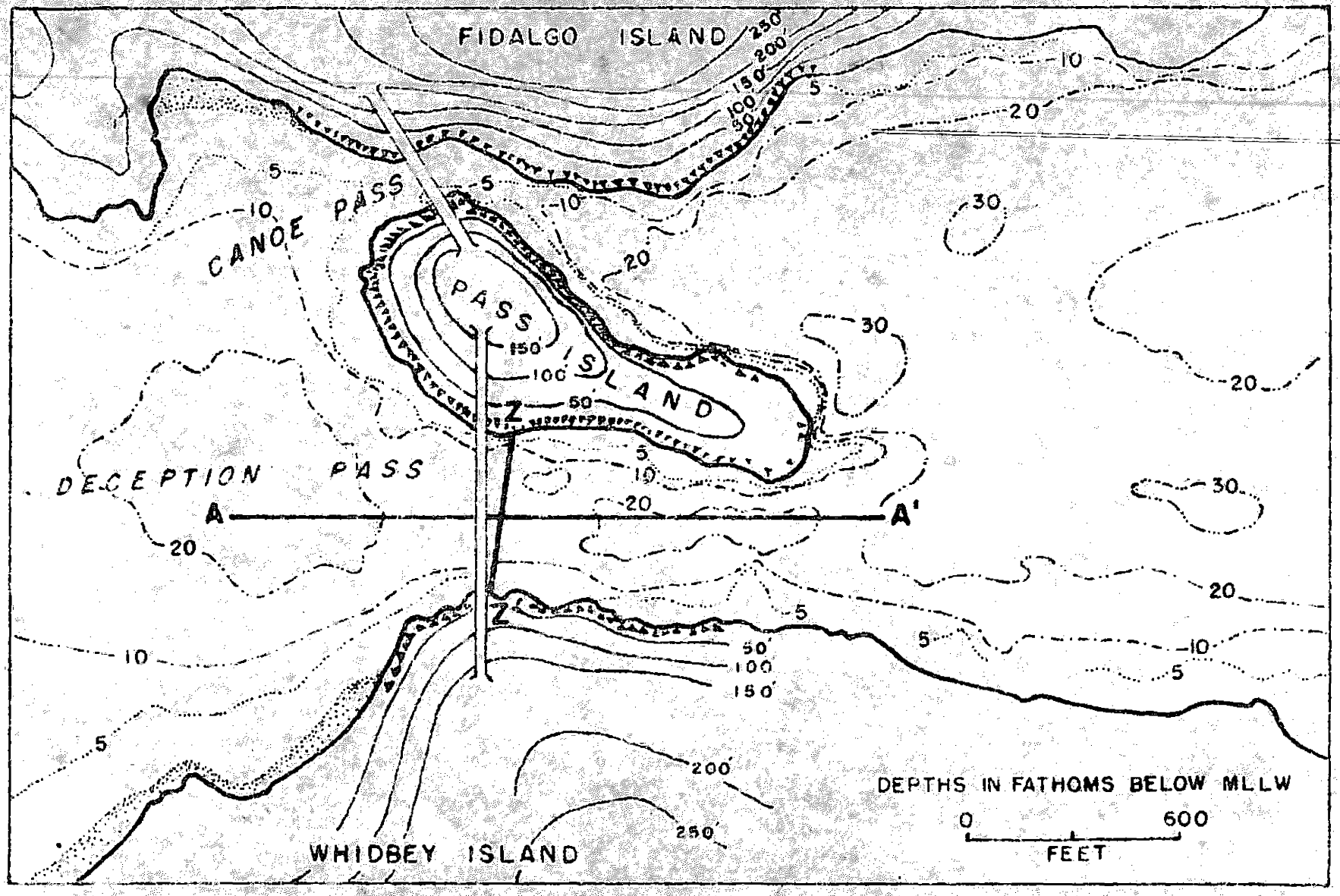

Figure 11. Plan of Deception Pass project site.

Transverse and longitudinal sections of the pass are shown in Figure 12. Superimposed upon the undistorted bottom profile of the pass, at the line of electrodes, is a semi-ellipse to which the pass section closely conforms. It was this feature that made the theory based upon an elliptical cross section particularly interesting. Several contour lines, both above and below the water surface, are shown in Figure 11 to indicate the slopes in this area.

The geology of the immediate area is very similar to that of other parts of Fidalgo Island described by McLellan (1927). The slopes of the pass, both above and below the water, are very steep and even above the water consist mainly of exposed solid rock. The rock of the cliff faces is a much-weathered basalt, very basic in chemical composition. The rock near the water has been analyzed and found to be a fine-grained gabbro, with many chlorites and some serpentines interspersed. The pass is less than 160 yards wide at the narrows and, as the geology of both sides appears to be identical, it is assumed that the rock structure at the bottom of the pass is the same as that of the sides. In view of the high water-velocities in the pass and the extreme turbulence, it is doubtful that any soft sediments cover the base rock in the narrows; it has been reported to the authors that the few bottom drags ever made through the pass have brought up nothing more than a few cobbles. Heiland (1952) gives specific resistivities for materials similar to those found in the pass area as:

Gabbro	$10^7 - 10^9$ ohm-cm
Serpentine	$10^4 - 10^6$ ohm-cm

For purposes of calculations, the specific resistivity was assumed as 10^6 ohm-cm for the pass.

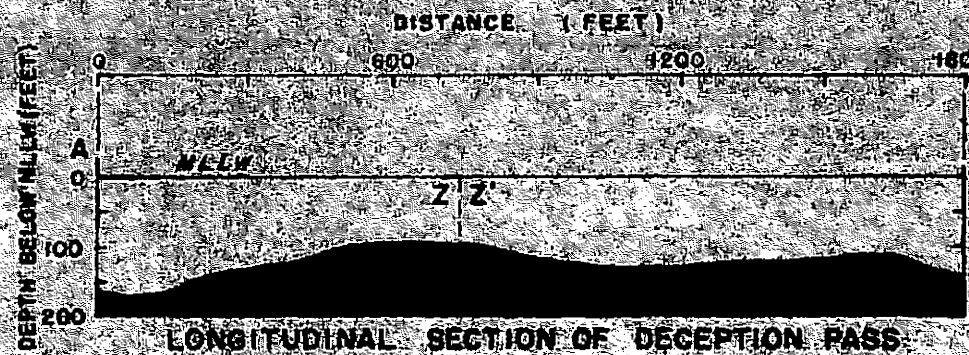

LONGITUDINAL SECTION OF DECEPTION PASS

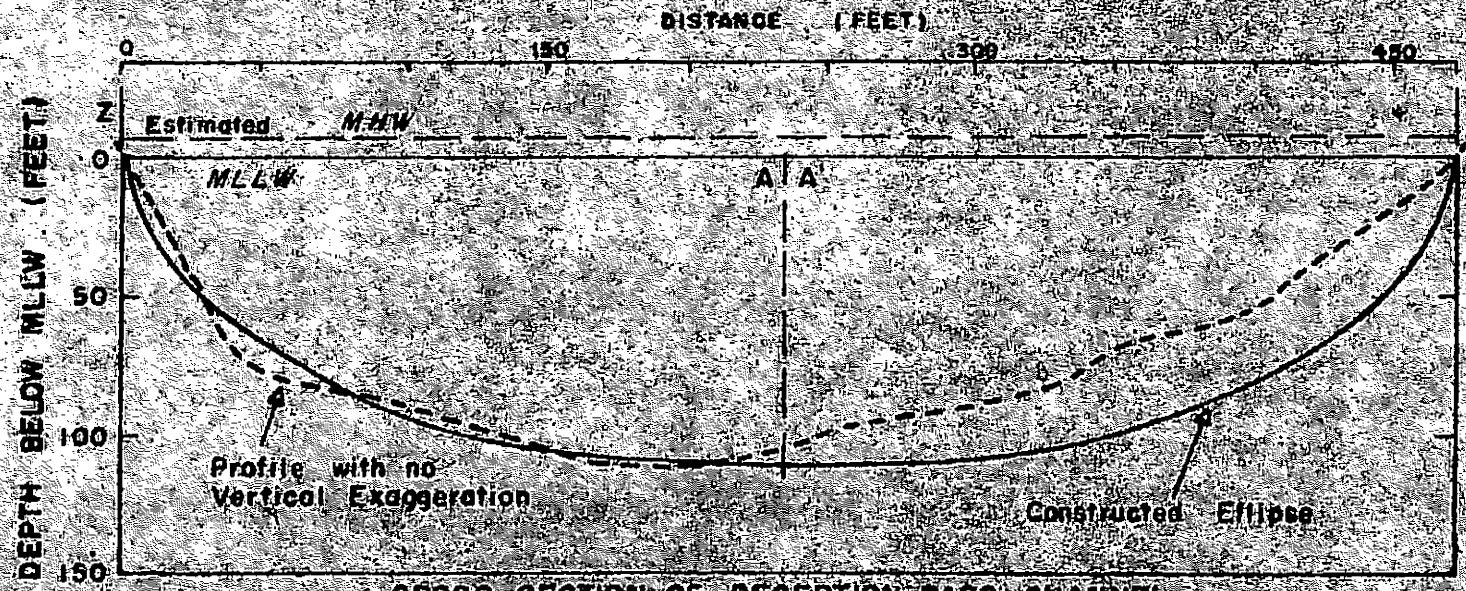

CROSS-SECTION OF DECEPTION PASS CHANNEL

Figure 12. Deception Pass sections.

3.2 Equipment

For the work at Deception Pass, the measuring circuit consisted of a Leeds and Northrup Speedomax Type G recording potentiometer, having an automatic standardizing cycle every 48 minutes. The rate of chart drive was 12 inches per hour, which was unnecessarily fast but unalterable. A special slidewire was used in conjunction with rewound shunting resistors to change the normal full scale of this instrument from ± 5 millivolts to ± 50 millivolts. The power supply was commercial 115 v. 60-cycle AC, used with a Raytheon voltage stabilizer. The recorder operated continuously for more than a month before a series of minor electronic failures left several major gaps in the continuity of the record.

The line of electrodes was located as nearly normal to the direction of current flow as access to the water's edge permitted. The solid-rock bottom did not allow the electrodes to be buried and, because the sheer slopes and the swirling waters prevented ready access to the water's edge from either direction, a simple arrangement of pendants was devised to permit the electrodes to be positioned satisfactorily and yet be readily removable for inspection, field zero checks, or replacement in case of damage. A sketch of the arrangement is shown in Figure 13. A heavy anchor was positioned several feet below MLLW; attached to the anchor was a 1-inch manila line which was led up the cliff face to a point of relatively easy access from the highway above. The shoreward end of the anchor line was secured to a stake or a small tree. The electrode housings were fitted with strong, brass eyelets through which the anchor line could be reeved loosely. With the anchor line held taut the electrodes could be slipped down the line,

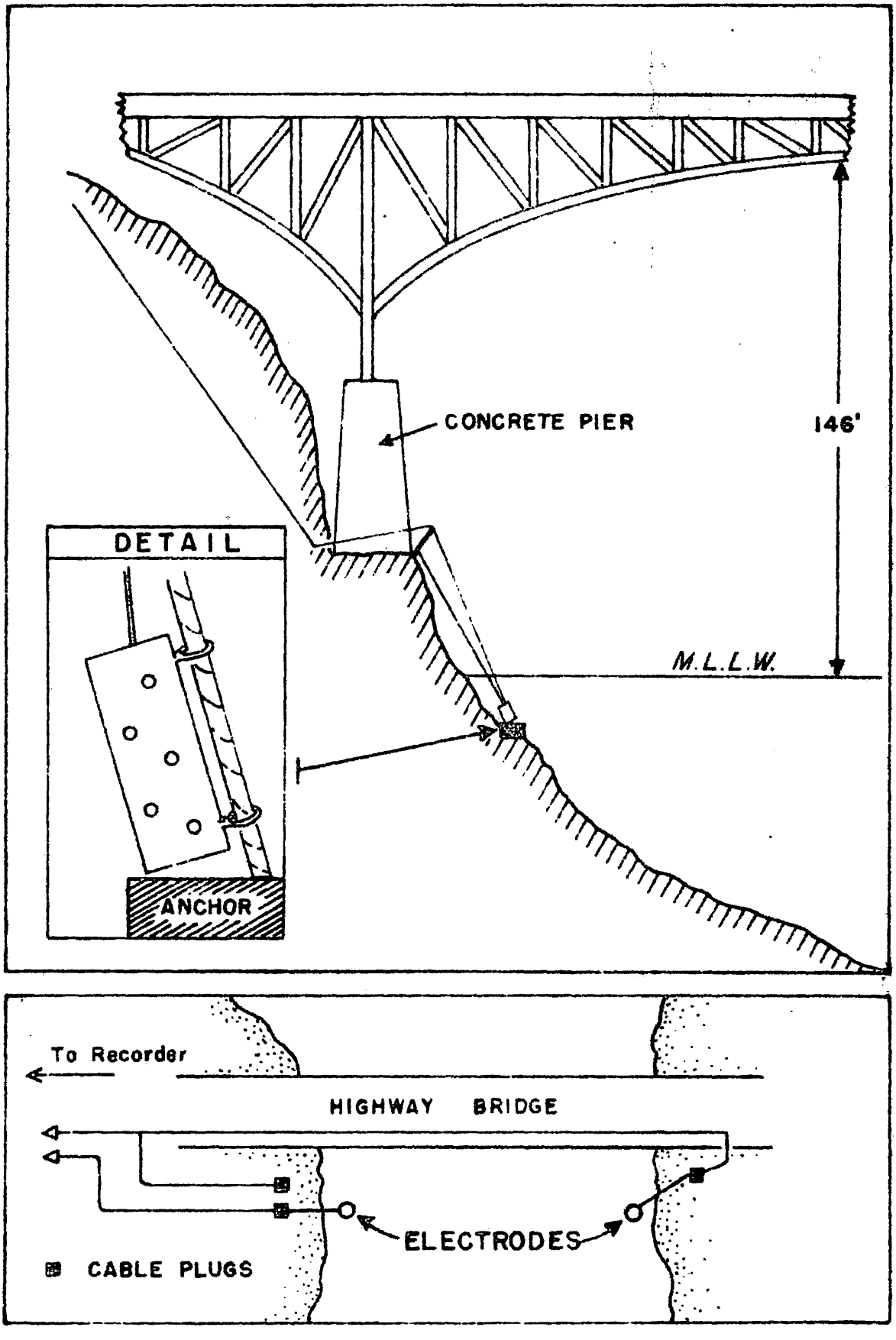

Figure 13. Electrode installations at Deception Pass.

the weight of their housings carrying them (with a little persuasion) until they eventually rested directly on the anchor; the anchor line and the cable were then secured. With 100-foot pendants of cable attached to the electrodes, the main cable installation led from the recorder to the vicinity of the upper part of the anchor lines, and cable plugs were used to complete the connections. This arrangement allowed one electrode to be removed from its location, carried to the other side of the channel with only a small amount of cable, positioned next to the other electrode, and connected to an auxiliary lead-in from the recorder while electrochemical zero was determined. Either electrode could then be taken back to the opposite side of the channel and the measuring operations could be resumed, all with no disturbance to the primary cable installation. The electrodes were checked because of their puzzling behavior during the Westcott Channel operations and because their exposed positions in Deception Pass left them vulnerable to damage from the debris carried by the stream. The necessity of this procedure was proved when, after three weeks of satisfactory operation, one of the electrodes was damaged and later another electrode was destroyed.

The recorder unit was located more than one-half mile south of the pass in one of the buildings of Deception Pass State Park, the closest source of commercial power. Highly flexible, heavily insulated cable was used for the electrode pendants, for the part of the installation which crossed the bridge, and for the first several hundred yards south of the bridge where the line of the cable led along the highway through a cut in the rocky slopes. Since the area is a tourist attraction, the cable was trenched-in wherever it crossed any trails, and also wherever it was exposed to the public view.

As protection against rock slides the cable at the foot of a rocky cliff was also trenched-in wherever the hard ground permitted. Field telephone wire was used for that half of the cable installation closest to the recorder. Where wire directly on the ground might later result in electrical leakage, it was strung from guard rails and tree bases with insulated staples. Point-to-point suspensions were closely spaced to eliminate potentials due to swinging loops of wire.

Equipment failures, some unavoidable, seriously handicapped the project after the first few weeks, and continuity of measurements was destroyed by large gaps in the record due to such failures. Some of the difficulties are listed below:

1. The cable was broken by rockslides on three separate occasions. On one occasion five breaks were found within 100 feet.
2. The cable was slashed completely through on one occasion by vandals.
3. Electronic failure of the recorder stopped the operation on four occasions; three of these failures were repaired in the field, while one required a shop check and the later replacement of the entire amplifier unit. A condenser in the recorder amplifier burned out, presumably when lightning struck near the highway bridge and sent a surge of induced high voltage into the recorder unit.
4. Many hours of record were lost due to a slightly damaged pen-tip which failed to print on several occasions.
5. One electrode was damaged by unknown causes during a period when electrode performances were not being checked.

6. One electrode was destroyed during a wind storm which reportedly created 6-foot waves in the pass. After this storm the anchor of the Pass Island electrode was found lodged in a niche in the cliff face several feet above the water line.

3.3 Tidal Currents and Velocity Distribution

The tidal currents of Deception Pass are mainly hydraulic, resulting primarily from differences in water level between the two ends of the pass. The tide to the east of the pass is basically mixed, whereas that to the west is more nearly diurnal. Daily tidal-height predictions are available (USC&GS) for a station about one mile east of the pass (Yokeko Point) and for a station less than a mile west of the pass (Reservation Bay). Checks by the Coast Survey indicate that the tidal height in the pass at any time is very nearly that which would be expected from the slope between the heights at the two reference stations. Figure 14 shows a composite plot of the tidal curves for the two reference stations during periods of both spring and neap tides. The observed times of zero and maximum potential during those days are noted on the plot.

The Coast Survey also publishes daily current predictions for Deception Pass, giving times of slack water and time and velocity of the currents at strength. Midchannel surface currents up to 10 knots are known in the Pass. The discharge of the many rivers and streams into northern Puget Sound, primarily that of the Skagit River, favors a net outflow or ebb through the pass. In 1925, while preparing for daily predictions in this area, the Coast Survey measurements indicated the net ebb-current through the pass as 0.65 knot.

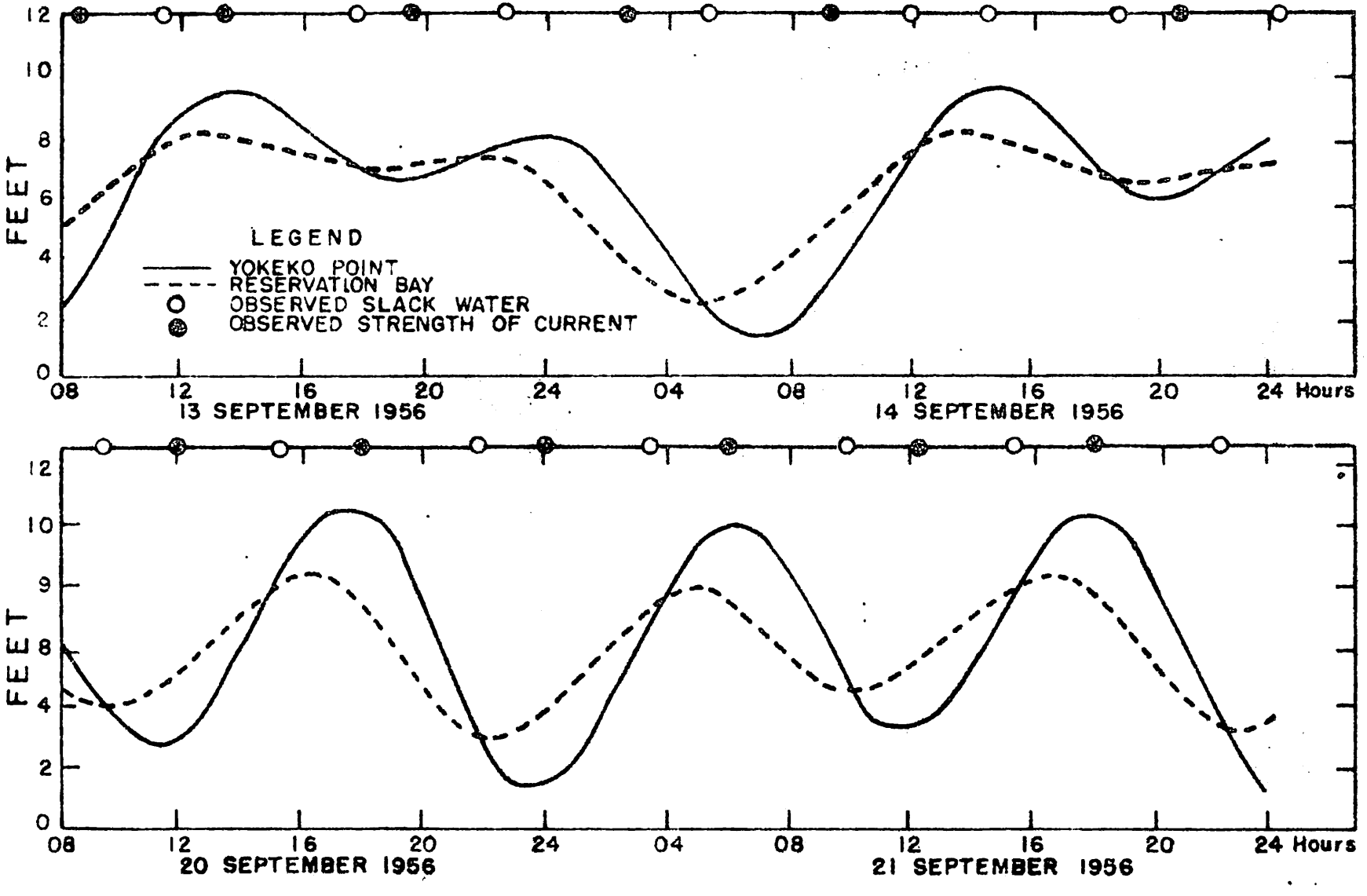

Figure 14. Tide curves of the reference stations at the extremities of Deception Pass.

The flow through the pass is characterized by visible turbulence at all but the lowest velocities. Some observations on the character of the turbulence, based upon data from electromagnetic observations, are included in Section 3.5.2. Because of the hydraulic nature of these currents, they are not sinusoidal but rather have a time-velocity relation of approximately $(\sin \frac{2\pi t}{T})^{\frac{1}{2}}$. This relation results in a very sharp fall and rise of the velocity profile through the slack-water point. Little is known about actual velocity distribution in the pass. It is not a suitable location for a vessel to anchor and measure currents,nor is it a location where radio current-meters could be positioned. Some velocity profiles have been measured about a mile from either end of the pass, but there is no assurance that these measurements have any significance in relation to actual distributions in the narrows. Visual observations show two critical velocities in the pass so far as turbulence is concerned: (a) one reached shortly after slack water and associated with the first appearance of eddies; and (b), a considerably higher velocity, apparently associated with a change of scale of turbulence. At this latter velocity the size of the eddies rapidly increases, vortices appear, and vertical upwellings sometimes raise the water level as much as a foot in the immediate area of such "boils". Trains of standing waves one or two feet in height have been observed stretching nearly across the channel, and it is reported that there have been times when the ocean swell has entered the pass and raised a single standing wall of water 30 feet high when met by the strength of the ebb. The authors failed to observe any occurrence similar to the latter, or to record potentials which may have been associated with this or any other anomaly of such magnitude.

3.4 Distribution of Temperature and Salinity

The difference between the physical and chemical characteristics of the waters of the flood cycle and those of the ebb cycle at Deception Pass are more marked than were the differences at Mosquito Pass or Westcott Channel. This is due primarily to the proximity of the Pass to the source of fresh water. To the west, the waters of Rosario and Juan de Fuca Straits are open directly to the North Pacific Ocean and exhibit many characteristics of oceanic water; Skagit Bay, to the east, is at times little more than a brackish lake. The greater part of Skagit Bay is very shallow, favoring local summer heating and local winter cooling. However, during the period September to November 1956, when the electromagnetic observations of this project were made, temperature differences were not prominent, the primary differences in the waters of the flood and ebb cycles through the pass being reflected in differences of salinity alone.

A few isolated measurements made early in the project in the vicinity of the electrodes showed only that the surface waters of the ebb were about 0.5° C. warmer and 2.0 °/oo less saline than the waters of the flood. Observations by the Department of Oceanography of the University of Washington in the vicinity of the pass (Stations 1 and 2, Figure 10) demonstrate the general situation, but are not truly synoptic. The composite data of Table 3 represent the extremes of the monthly observations obtained at these stations during the months of October and November during the three-year period 1952-1954. During flood stage of the Skagit River the difference in surface salinity between the two stations was as great as 12 °/oo in January 1952.

Table 3. Extreme temperatures and salinities observed off the outer and inner entrances to Deception Pass during the months of October and November, 1952-54

Station 1			Station 2		
Depth (meters)	T(°C)	S(°/oo)	Depth (meters)	T(°C)	S(°/oo)
0	8.80	30.97	0	9.50	26.74
5	8.75	30.97	5	9.50	27.43
10	8.77	30.99	10	9.50	27.77
20	8.70	31.02	20	9.50	28.43
30	8.75	31.08	30	9.40	29.69
50	8.75	31.15	--	--	---
75	8.68	31.18	--	--	---

The large, transient changes in salinity which may occur along the pass are not likely to result in concentration cells across the pass because of intensive mixing. However, it is vital that the electrochemical stability of the electrode-pair be assured throughout the salinity range encountered.

The Skagit River usually has two periods of maximum discharge: one in the late fall or early winter due to seasonal rainfall, and another in the spring due to snow melt in the watershed. These maxima are commonly of the order of 60,000 to 100,000 ft^3/sec (1700-2800 m^3/sec). It might be of interest to note that if Skagit Bay were sealed off at Deception Pass and at its juncture with Saratoga Passage, such river-discharge rates would be sufficient to raise the water level of the "lake" 4 to 6.5 meters per day.

3.5 Observations and Calculations

3.5.1 Comments on the record of measured potentials

Observations of electromagnetically-induced potentials at Deception Pass were obtained over a period of 2½ months (from 0000 hours, 13 September 1956, to 1930 hours, 20 November 1956). The period from 13 September to 7 October was one of the longest periods of uninterrupted operation and was the only period during which the observations are believed to be free from error. Error is known to have existed in all operations subsequent to 7 October, although in many cases it is felt that the existing error could be satisfactorily estimated to provide corrected data. However, inasmuch as the certainty of the corrections cannot be guaranteed, the observation period is divided as follows:

23 days of reliable observations,

19 days of conditionally acceptable observations,

11 days of unreliable observations, and

24 days during which no observations were obtained.

Field checks of electrochemical zero were made on four occasions during the first week of operation, and once at the end of the second week of operation. The checks were made at various stages of both the flood and ebb cycles, and at no time was an electrochemical potential in excess of 0.3 millivolt noted. The linearity of the measuring circuit was satisfactory when checked by calibration of recorded potentials against known input voltages.

3.5.2 Observation on turbulence

Early in the project it was noted that short-period variations or irregularities in potential occurred during periods of sufficiently large velocity. Figure 15 shows two sections of the original record obtained on the morning of 1 October 1956, characteristic of the respective types of record.

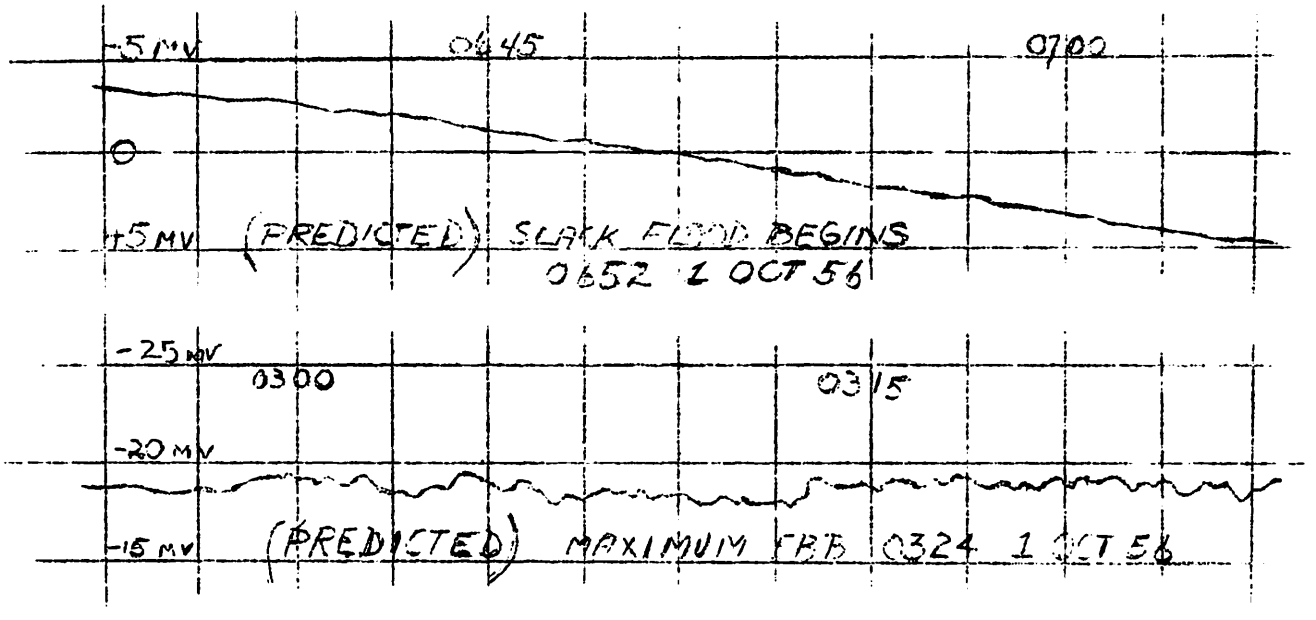

Figure 15. Deception Pass record showing absence and presence of "turbulence".

Because of previous fluctuations in potential with surges and turbulence such an association was immediately sought here, but visual observations of the flow patterns in the pass confirmed the fact that considerable turbulence existed long before irregularities of potential appeared on the record. However, the appearance of the irregularities on the record was very nearly concurrent with the appearance of vortices and upwellings in the pass. The hypothesis advanced here is that, in a certain

critical range of velocities, the character of the turbulence in the pass is changed. The small-scale turbulence present in the pass at moderate velocities averages-out across the channel and does not influence the potential-gradient developed by the mean motion of the flow through the channel. At higher velocities, the character of the turbulence changes in a manner which no longer allows the mean motion to remain unaffected by these variations.

An analysis of the record of approximately 25 ebb-and-flood cycles, during which the appearance and disappearance of the irregularities was relatively clear-cut, yielded the following average values (the factor of 2.42 mv/kn is used to change units of potential to units of velocity):

ebb velocity at which "turbulence" appeared	5.0 knots
ebb velocity at which "turbulence" vanished	4.1 knots
flood velocity at which "turbulence" appeared	5.4 knots
flood velocity at which "turbulence" vanished	4.5 knots

From a "turbulence" hypothesis, it would be expected that higher velocities would be necessary to establish large-scale turbulence than would be required to maintain such turbulence, once established*. No attempt is made to explain the differences between flood and ebb critical velocities, in part because individual comparisons themselves show differences up to 1 knot.

3.5.3 Theoretical potentials

In the planning stages of the Deception Pass project a calculation was made, based upon the theory of Longuet-Higgins (1949), to estimate the

---

* A tendency which seems to be supported by the data.

maximum potential which might be expected during the observations to be made at the pass. Assuming an elliptical channel, a perfectly insulating channel-bed, and a uniform velocity, and with

V_{max} = 10 knots

H_z = 0.536 gauss

x = 144 meters

it was found that

$\frac{\partial \phi}{\partial x}$ = 2.76 x 10^{-6} volts/cm,

and

ϕ = 39.6 millivolts.

The assumption of a nonconducting channel-bed is particularly free from error in this case. Following the notation of Longuet-Higgins et al., (1954) with:

a = 72 meters, ρ_1 = 30 ohm-cm (T = 10° C, S = 30 °/oo),

b = 33 meters, ρ_o = 10^6 ohm-cm,

the effect of the actual conductivity of the channel-bed reduces the theoretical potential by the factor 1.000066.

Thus, the induced potential in the pass was estimated at

$$\frac{\phi}{VL} = f = 27.5 \text{ mv/kt/km.}$$

3.5.4 Basis of the velocity-potential calibration

As the environmental conditions in the pass during the first 23 days were relatively uniform and the uninterrupted observations were believed free from error, this period was utilized as the calibration period. The electromagnetic data were calibrated with the use of predicted velocities

(midchannel, subsurface) for the pass narrows since it is not feasible to determine horizontal and vertical velocity profiles in the pass by direct measurement. Therefore, the calibration is not a direct determination of the transport-potential relation nor the mean velocity-potential relation. This in no way implies, however, that qualitative, or even quantitative, information of transports in the pass cannot be obtained.

The first attempt at calibration was based upon the velocity-potential relations observed at the strength of current only. The largest measured potential obtained during any cycle, turbulent irregularities being averaged, was compared to the predicted strength velocity for the same cycle. This particular method of calibration allowed the use of tabular values of the velocity predictions rather than requiring that velocities be read from the special scale of the marigram. More important, this was a comparison of maximum values without regard to small differences in the time of their respective occurrences. Current velocities from the marigram at a time other than strength of current compared with concurrent potential would require that the time of slack water and zero potential be almost identical in order to avoid an offset relation.

Since the calibration was to be made against predicted velocities, it was first necessary to ascertain the basis of the predictions. A series of personal communications with Rear Admiral Robert W. Knox, Assistant Director of the United State Coast and Geodetic Survey, revealed the following information as to the prediction of current velocities in Deception Pass:

1. The tabular values of the predicted current velocities, as they appear in the Pacific Coast Current Tables, are for a position slightly subsurface at midchannel in the narrows of the pass.

2. Since the currents are primarily hydraulic, the velocity may be expressed as $V = (kh)^{\frac{1}{2}}$, where h is the differential hydraulic head between the two ends of the pass, and k is a constant.
3. From tidal observations at Reservation Bay and Yokeko Point (Stations A and B, Figure 10) harmonic constants were derived from which the head (h) could be predicted at any time. Head measurements were taken during the period of current observations and found to agree with predicted head.
4. The determination of the constant (k) was empirical. Current observations were made by use of current-buoys for a 3-day period (6 floods and 6 ebbs) at a location just off the southeast end of Pass Island. During these observations, measured flood velocities ranged from 4.8 to 5.7 knots and measured ebb velocities from 5.2 to 7.8 knots. An average value of 5.9 knots was used to change units of "head" to units of "velocity".
5. Thereafter, they used predicted water-level differences to develop a formula for the prediction of current velocities. The current-velocity curve was then drawn by machine and the scale of this marigram is given by

$$V \text{ (knots)} = -0.65 \pm \left(\frac{80}{3} d\right)^{\frac{1}{2}},$$

where d is the ordinate of the marigram in inches. The sign of the last term is positive for flood current and negative for ebb currents. The constant, -0.65 knot , represents the estimated net surface-ebb current through the pass.

3.5.5 The velocity-potential calibration

When the velocity-potential relation was plotted for several cycles it became apparent that the calibration factor was not a constant but was a function of the absolute value of the predicted velocity (Figure 16). The points on this curve represent comparisons for the entire calibration period, the symbols for the various points differentiating between data obtained on the flood and ebb cycles. No statistical evaluation was made, the line curve representing merely the authors' estimate of the best line through the point.

Some of the possible reasons why the relationship between the induced potentials and predicted surface velocities are not constant are given below:

1. The existence of systematic errors in the measured potentials
2. The non-existence of any constant relation between the surface velocity and the transport of the stream
3. The non-existence of any constant relation between induced potential and transport
4. The existence of systematic errors in the predicted velocities.

None of these possibilities can be entirely ruled out. Inspecting each in order it is found that:

1. The existence of systematic errors in measured potentials, while possible, is doubtful. The calibration period was chosen as being representative of the best data obtained, and the calibration curve is the result of data from almost 100 individual observations. In addition, errors which might be inherent in the measurement of potential would not tend to be systematic, except perhaps in the instrumentation, and checks of the measuring circuit had shown the recording-potentiometer to be linear.

Figure 16. The velocity-potential relation at Deception Pass as a function of velocity.

2. It is not only possible but probable that there is a variable relation between surface velocity and transport. With transport representing the numerical product of an instantaneous mean velocity and the cross-sectional area of the stream, a surface velocity-transport proportionality would require a near-constant ratio of surface and mean velocities, compensated for in some way by the time variation in the cross section of the stream. Since, during any cycle the currents in the pass were observed to exhibit markedly different types of flow (laminar flow as well as two separately characterized turbulent flows), it is virtually impossible for the relation of mean velocity to surface velocity to be a constant. No attempt will be made here to put numerical limits on the range of variability of the factor $\bar{V}/V_s$, not even to the extent of describing the factor as always less than unity.
3. It has been shown (Morse, 1957) that the transport-potential relation is dependent upon the velocity distribution functions, and it is probable that these functions are dependent upon the magnitude of the velocity, or at least upon certain ranges of the velocity (within which the distribution might remain relatively constant).
4. With regard to the possibility of systematic error in the predicted current velocities, predictions of this nature are designed primarily for the use of navigators and, as such, the most important considerations are the times of slack water and the times and velocities of strength of current. The degree of precision of predictions of this type is always open to question, due to the very nature of the calculations involved (see Section 3.5.4).

In the case of the predictions at Deception Pass, the precision of the predictions does not necessarily represent that required for the study of net water exchange. Indeed, the variation of the Deception Pass calibration readily lends itself to an association with a systematic error, if any, in the predictions. For instance, if it is assumed that the calibration should be constant (that is, if it is assumed that the surface velocity has a constant relation to the average velocity of the stream) and if it is assumed that the potential is directly proportional to the transport, the slope of the actual calibration curve seems to become explainable on the basis of systematic errors in the predictions. Describing the currents in the pass as completely hydraulic and using the "square law" for predictions requires that the effect of accelerations and the time-dependence of the motion be neglected. Since the predictions are based upon observations at strength of current, it is reasonable to neglect accelerations at these maxima, but at intermediate velocities this term is not necessarily negligible. There may be times, particularly during periods of low velocity, when the acceleration term becomes very important. Therefore, while the predicted velocities may be quite accurate within the range of velocities upon which the predictions are based, there is no assurance that the empirically-determined constant (k) holds throughout the entire velocity range. In addition, the difference between the net flow and its predicted value will affect the calibration.

3.5.6 A practical transport-potential calibration

To obtain a useful, constant calibration for Deception Pass it is first considered that for surface velocities in the vicinity of 5.9 knots, the velocity upon which the predictions are based, the predicted velocities are without appreciable error barring anomalous conditions in the pass area. Further, observations have indicated that velocity distributions are relatively constant for velocities of this magnitude as well as being very nearly the same for both the flood and ebb cycles. Assuming that, within a moderate range of surface velocities centered about 5.9 knots, the surface velocity has a constant relation to the mean velocity (transport) and that within this same range the potential has a constant relation to transport, then the velocity-potential calibration may be shifted to a transport-potential calibration at this point. A second reference point is yielded by the knowledge that zero transport should result in zero potential. On a plot of potential against transport the line joining the two reference points represents the transport-potential calibration, assumed linear. This is the best single calibration consistent with available information.

Therefore, assuming the ratio of mean velocity to surface velocity as 0.75 and with the average cross-sectional area of the pass (taken at midtide at the line of electrodes) as 3540 m^2, predicted surface-velocities can be related directly to transports. Figure 17 represents a composite plot of the velocity-potential and transport-potential calibrations. To fill in the somewhat vacant low-velocity range, several days of observations were chosen when the time of zero potential actually occurred within 3 minutes or less of the predicted times of slack water, and low-velocity predictions were read off the marigram and plotted against concurrently measured potentials.

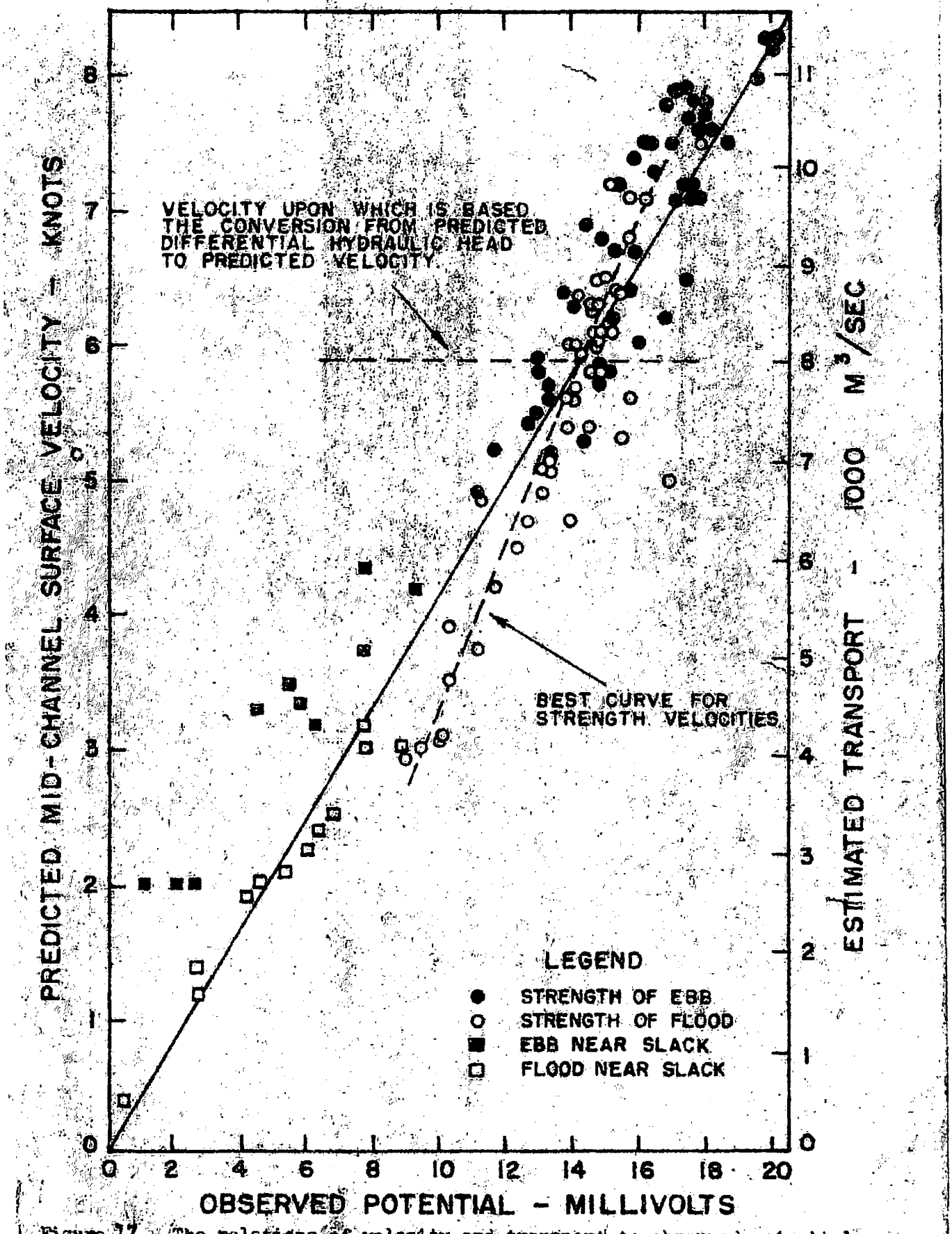

Figure 17. The relations of velocity and transport to observed potential at Deception Pass.

The respective ebb and flood "calibrations" are distinctly separated in this velocity range. Intermediate velocities tend to follow the transport or "mean velocity" average calibration rather than the maximum velocity calibration.

The following relations best represent the data from Deception Pass:

$$\text{midchannel surface-velocity at strength (kts)} = \frac{\phi^{mv} - 4.6}{2.19}$$

$$\text{intermediate midchannel surface-velocity (kts)} = \frac{\phi^{mv}}{2.42}$$

$$\text{transport } (m^3/\text{sec}) = 565\ \phi\ (mv)$$

SECTION 4

TRANSPORT IN DECEPTION PASS AS RELATED TO METEOROLOGICAL FACTORS AND RIVER RUNOFF

4.1 General Considerations

It was known that fresh-water runoff into the embayment systems east of Deception Pass resulted in a net ebb flow through the pass. If the average net transport through the pass is assumed to be given approximately by

$$\bar{T}_n \approx k\, V_p\, \bar{A},$$

where: V_p = the predicted net surface ebb current through the pass given in Section 3.5.4 as 0.65 knot (0.334 m/sec),

$\bar{A}$ = the average (midtide) cross-sectional area of the pass at the narrows, 3540 m^2,

k = 0.75, an approximation of the factor $\bar{V}/V_{max}$,

then

$$\bar{T} = 890\ m^3/sec$$

$$= 77 \times 10^6\ m^3/day.$$

Measured net ebb transports were calculated from the electromagnetic data by numerically integrating the potentials over a completed tidal-day, and converting to units of transports by use of the calibration (f) of Section 3.5.6 and the factors $\bar{A}$ and k as used immediately above. Thus

$$T_n \approx \frac{k\bar{A}}{fT} \int_0^T \phi\, dt$$

and the anomaly of transport is $T_n - \bar{T}_n$.

4.2 The Relation of Runoff to Net Ebb Transport

Since it may be assumed that the discharge of the Skagit River is partly responsible for the net outflow through Deception Pass, it was considered that changes in the discharge rate of the river would be reflected in changes in the measured net daily ebb through the pass. Net daily ebb-transports were approximated from electromagnetic data as indicated in Section 4.1. The daily discharge of the river was computed from river-gauging records made available by the Water Resources Division of the Geological Survey (U. S. Department of the Interior). Figure 18 represents a summary plot of the discharge and transport calculations.

The lack of continuity of the electromagnetic data prevents any satisfactory comparison between the two records; however, a certain qualitative agreement between the curves is shown in that the larger net ebb-transports are generally associated with higher river-discharges. Although of questionable justification, a quantitative relation may be attempted if it is assumed that the rather well-defined fluctuations in river discharge which took place between 27 September and 2 October are responsible for the somewhat similar variations in net transport observed between 2 and 6 October. On this very tenuous ground, it would appear that there is a lag of approximately 4 days between the time a marked change occurs in the river discharge and the time at which that change is reflected in the net transport through the pass. Further, throughout most of the early weeks of observation the net transport remained nearly twice the value of the river discharge. If the principle of conservation of salt is employed in conjunction with this 2:1 relation of volumes, an extremely approximate calculation (salinity

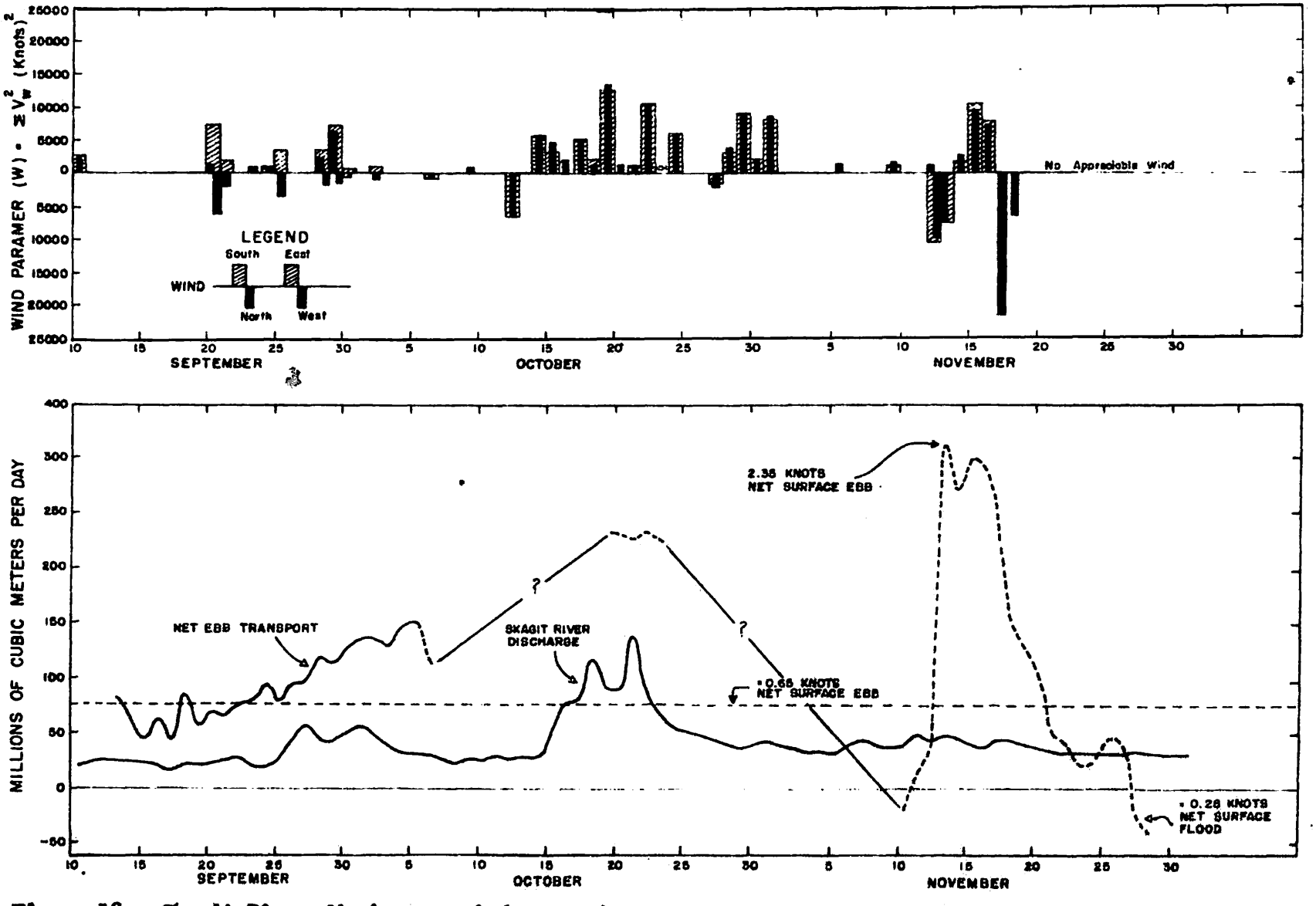

Figure 18. Skagit River discharge, wind parameters, and net transports in Deception Pass; September - November, 1956.

of ebb transport assumed to average about 2 °/oo less than the salinity of the flood transport) indicates that even at moderate river-level about 20 per cent of the ebb transport is made up of Skagit River water.

4.3 The Relation of Wind Effects to Net Transport

Two hypotheses were investigated on the effect of winds. These were based on the assumption that winds of sufficient velocity and duration over water surfaces adjacent to the pass area would influence the surface slopes to a degree which might result in anomalous hydraulic heads at the pass, and hence anomalous net transports.

The first hypothesis was that south winds over the Saratoga Passage - Skagit Bay system would tend to pile-up water in the vicinity of Yokeko Point, increasing the head at the east end of the pass and resulting in an increased net outflow through Deception Pass, the lone outlet from the northern part of the bay system. Winds from the northern quadrant would tend to have the opposite effect. The effect of north-south winds on sea level west of the pass was neglected on the assumption that any surface-slope created in this area would be rapidly dissipated by water motions through the larger straits and channels.

The second hypothesis was that the limited fetch over the interior waters would cause north-south winds to be less important than east-west winds blowing over the much greater fetch of the Strait of Juan de Fuca. These winds could influence sea level to seaward of the pass, and could even pile water directly into the western end of the pass.

"Surface"-wind data was obtained from recorded observations made at the U. S. Naval Air Station, Whidbey Island, located about 7 miles south of

Deception Pass; and from the U. S. Air Force Base, Paine Field, located some 30 miles south of the pass and directly in line with the southern reaches of Saratoga Passage. The normal wind-distribution patterns for northwestern Washington and southwestern British Columbia, as described by Harris (1954), were used to relate individual station data to the probable over-all wind field.

No actual calculation of wind stresses or slopes could be made from the amount and type of data available, but a parameter was invented to permit some form of calculation allowing qualitative comparison. Reported wind velocities were averaged throughout each hour, squared, grouped by direction according to whether the north-south or east-west effects were desired, and then summed for each day. Wind velocities less than 12 knots were not considered. The magnitude of the sum indicated the combined effect of the velocity and the duration, while the direction was indicated by algebraic sign. Since a net ebb-transport through Deception Pass was considered "normal" and thus plotted as "positive" in Figure 18, south and east winds were assumed to be "positive" in that they were assumed to increase the net ebb-transport, whereas north and west winds were assumed "negative". For example, a wind that blew from the south at 15 knots throughout an entire day, would have wind parameters as follows:

$$W_{n-s} = 24 \times (15)^2 = 5400,$$

$$W_{e-w} = 0,$$

and the wind parameter for this day would appear only once on the graph. If the wind had blown from the southwest throughout the day, also at 15 knots, the wind parameters would then be:

$$W_{n-s} = 24 \times (15)^2 = 5400$$

$$W_{e-w} = 24 \times (15)^2 = -5400,$$

and the parameter for this day would appear twice on the graph, once positive and once negative. Inasmuch as the four cardinal directions are incorporated into the data, the predominant wind direction for any day can be determined by relating the numbers and signs of the wind parameters which are shown for that day.

It is found that the discontinuity of the electromagnetic data is such that it is possible only to speculate as to the relationship that might exist between net transport and winds. During the $2\frac{1}{2}$-month observation period there were two marked periods of prolonged, high-velocity winds. The first occurred during a period in which no electromagnetic observations were obtained, and the second occurred during a period in which the electromagnetic observations are only conditionally acceptable (Section 3.1).

The record from 13 September to 6 October reveals that the variations in net transport cannot be ascribed to either runoff or winds. The record for the month of November, a period during which the runoff was very uniform yet the variation in net transport was extreme, suggests only that prolonged, high-velocity winds presumably do have a marked effect on the net transport. It is further suggested that the effect of the sudden cessation of strong winds is just as marked. This latter observation, if justified, suggests that there may be a very important relaxation phenomena associated with variations in wind stresses on the waters of this area.

4.4 Additional Comments on Net Transports

Since it is not the purpose of this report to thoroughly investigate the relationship of Deception Pass transports to any single factor, it remains only to point out that influences other than runoff and wind are probably important.

For instance, differences in sea level between the east end of Deception Pass and the southern reaches of Admiralty Inlet may be a major factor. Such differences could be related to local gradients of atmospheric pressure, or even to wind-stress slopes, on a somewhat different basis than previously discussed. Deception Pass nevertheless represents only about 2 per cent of the total tidal transport of the Puget Sound system, and small changes in the Admiralty Inlet dynamics might be reflected by large anomalies at Deception Pass.

Further, each fall "dense water" from the ocean flows through Admiralty Inlet to displace the bottom waters of Puget Sound, which in turn discharge at lesser depth. This resulting increase of outflow in the upper layers would favor a net ebb through the relatively shallow Deception Pass, and contribute to the anomalous high ebb observed there during November 1956.

SUMMARY AND CONCLUSIONS

5.1 Summary

Perhaps the best way to summarize the various data presented in this report is to compare the velocity-potential calibrations of the project areas, both as to differences between calibrations determined for the respective areas and as to individual differences between actual and theoretical calibrations. Where possible, reasons will be suggested for these latter differences. Similar data from other areas, as reported by other investigators, is presented for purposes of comparison. Theoretical calibrations were made from the theory of Longuet-Higgins (1949). In all cases the channels were considered to be of elliptical section and the water velocity was assumed to be uniform.

5.1.1 Westcott Channel - Mosquito Pass

Direct calibration of Westcott Channel was performed by comparing observed potentials to transports determined directly by calculation of the time-rate change of tidal-prism volumes. The channel-bed resistivity of Westcott Channel was assumed to be 10^4 ohm-cm. The theoretical and observed calibrations are respectively:

$f = 26.0$ mv/kt/km, and $f = 15.4$ mv/kt/km.

The difference between the two calibrations is thought to result from the complex velocity distributions in the channel, and from "edge effect" losses because of the shape and size of the channel.

No direct calibration was obtained for Mosquito Pass. The assumption of a perfectly insulating channel-bed leads to the theoretical calibration

$f = 27.5$ mv/kt/km.

5.1.2 Deception Pass

No direct comparison between actual and theoretical calibrations is made for Deception Pass because the theoretical calibration is based upon an integrated or mean velocity, whereas the direct calibration was based upon a surface velocity. The assumption of a perfectly insulating channel-bed yields a theoretical calibration of

$$f = 27.5 \text{ mv/kt/km (mean current).}$$

The direct calibration, as presented in Section 3.5.6, was found to be

$$f = 16.8 \text{ mv/kt/km (surface current).}$$

Assuming the factor $\bar{V}/V_{max}$ as any factor less than unity would tend to bring the two calibrations closer together. If the losses in measured potential due to the edge effects, which latter are presumably very great in this case because the channel is so narrow and deep, could be accounted for, these also would bring the calibrations closer together. No doubt other errors in the calibration result from the relatively short length and the non-uniformity of the channel. It has been suggested that some loss of measured potential might be due to electrical leakage through the highway bridge which spans the channel. Although this seems highly doubtful as the bridge is supported upon concrete piers resting upon very high-resistivity rock well above the water level, it has not been disproved and thus remains a possible source of error.

5.1.3 Comparative data

A condensed tabulation of the project data is shown in Table 4 together with data from other investigations. Where both are known, theoretical and direct calibrations are presented. The difference between the two calibrations is generally indicative of the inability to describe actual channels, velocity distributions, etc., by simple theory.

Table 4. Comparative mean velocity-transport calibrations

Observer	Location	Calibration (f) (mv/kt/km) Theoretical	Direct
Morse	Mosquito Pass	27.5	- -
"	Westcott Channel	26.0	15.4
"	Deception Pass	27.5	22.4 (1)
Pickard and Lyon	Bering Strait	11.0	0.5-2.0
Bowden	English Channel (2)	- -	3.2
"	English Channel (3)	- -	10.6

(1) $\bar{V}/V_{max} = 0.75$
(2) Section at Aldeburgh-Domburg
(3) Section at St. Margaret's Bay-Sangatte

5.2 Conclusions

The common objective of the individual projects was to determine if the electromagnetic method was a practical method for the measurement of transport in small tidal streams. The very fact that transports are being maesured in such places as the Bering Strait, the English Channel, and the Gulf Stream indicates that the method, while not perfected, is of practical value as an oceanographic tool in large streams. However, the fact that the measurement of induced potentials can be related to transport in large streams in no way assured that the method would prove practical if applied to smaller streams. Even the theory suggests that the problems and variables to be encountered in application of the method to a narrow, deep channel will be greatly different from those encountered in a wide, relatively shallow channel. However, if the method could be proved on a very small scale,

then it could be reasonably assumed that the method, already proven for large streams, would prove satisfactory at any intermediate scale. The term "small-scale" is, of course, relative and as used here is a field term. Actually, methods using the principle of electromagnetic induction have been used on very small-scale projects such as measuring the flow in models and pipes (Kolin, 1945) and even in measuring the flow of blood through the veins of the human body (Kolin, 1936).

The major conclusion of this work is that the electromagnetic method is capable of providing easily obtainable, accurate, and continuous measurement of transports and/or velocities (depending upon the basis of calibration) in tidal streams of any size or configuration. The primary factors in the successful application of such a method are:

1. Elimination or reduction of electrochemical errors
2. A high standard of accuracy, stability, and durability in the various components of the instrumentation to provide continuity of record
3. A sufficient understanding of the electromagnetic theory as applied to any particular stream to provide insight into the many variables and their affect on the measured potentials
4. The determination of a suitable calibration factor, or factors, by application of (3) so that the calibration is performed over a satisfactory range of variables.

Insofar as the specific projects of this work are concerned, it is concluded that:

1. Electromagnetic measurements in small streams are particularly in need of a high standard of control. It is not necessary to be overly concerned with the fact that the general theory is not conducive to direct application to narrow, deep streams, since the method will probably require actual calibration in the field before it can be used. However, because the total potentials developed in small streams are necessarily also small, minute errors due to cell effects, variable electrical losses, unmatched electrodes, and stray potentials cannot be averaged or neglected as they often can be with total potentials of greater magnitude.
2. While no definite statements can be made as to the relation of meteorological effects and runoff to the net transport of Deception Pass because of the meager data available, it is evident that these relations could be supplied by further studies based upon electromagnetic principles.

REFERENCES CITED

Barnes, C. A. et al.
1956. Preliminary oceanographic report of channels through the San Juan Islands between Fidalgo and Vancouver Islands. Univ. Wash. Dept. Oceanogr. Spec. Rep. 21, Ref. 56-3, 137 pp.

Bloom, G. L.
1956. Current, temperature, tide, and ice growth measurements, Eastern Bering Strait - Cape Prince of Wales, 1953-55. U. S. Navy Electronics Lab., San Diego, Res. Rep. 739, 25 pp.

Bowden, K. F.
1956. The flow of water through the Straits of Dover related to wind and differences in sea level. Philos. Trans., Series A, No. 953, 248: 517-551.

Faraday, Michael
1832. Terrestrial magneto-electric induction. The Bakerian Lecture, Art. VI, Experimental researches into electricity, 2nd series, Sec. 5. Philos. Trans., Part I: 163-177.

Harris, Russell G.
1954. Surface winds over Puget Sound and the Strait of Juan de Fuca and their oceanographic effects. Thesis, Univ. Wash., 76 pp.

Heiland, C. A.
1946. Geophysical exploration. Prentice-Hall, Inc., New York. 1013 pp.

Helle, James R.
1955. Currents in Mosquito Pass. Unpubl. manuscript, Univ. Wash. Dept. Oceanogr., 23 pp.

Kolin, A.
1936. An electromagnetic flowmeter. Principle of the methods and its application to bloodflow measurements. Proc. Soc. exp. Biol. and Med., 35: 53-56.

Kolin, A.
1944. Electromagnetic velometry. I. A method for the determination of fluid velocity distribution in space and time. J. appl. Phys., 15(2): 150-164.

Levin, H., and C. F. Bonilla
1951. Thermogalvanic potentials. J. electrochem. Soc., 98: 388-394.

Longuet-Higgins, M. S.
1949. The electrical and magnetic effects of tidal streams. Mon. Not. Roy. Astr. Soc., Geophys. Suppl., 5(8): 295-307.

Longuet-Higgins, M. S., M. E. Stern and H. Stommel
1954. The electrical field induced by ocean currents and waves, with applications to the method of towed electrodes. Pap. phys. Oceanogr. Meteorol., 13(1): 1-37.

McLellan, R. D.
1927. Geology of the San Juan Islands. Univ. Wash. Publ. Geol. 185 pp.

Morse, Richard M.
1957. The measurement of transports and current velocities in tidal streams by an electromagnetic method. Thesis, Univ. Wash., 134 pp.

Olsson, B. H.
1955. The electrical effects of tidal streams in Cook Strait, New Zealand. Deep-Sea Res., 2: 204-212.

Pickard, G. L. and W. K. Lyon
1949. Attempted electromagnetic measurements of sea currents in the Bering Strait. Canad. Joint Comm. on Oceanogr., Pacif. Ocean Group (Project Aleutians), 16 pp. + appendices.

Von Arx, William S.
1950. An electromagnetic method for measuring the velocities of ocean currents from a ship underway. Pap. phys. Oceanogr. Meteorol., 11(3): 1-61.

Wertheim, Gunther K.
1954. Studies of the electrical potential between Key West, Florida, and Havana, Cuba. No. II. Woods Hole Oceanogr. Instit., Ref. 54-68, 17 pp.

Department of Oceanography
University of Washington

UNCLASSIFIED TECHNICAL REPORT DISTRIBUTION LIST

3 Chief of Naval Research
Department of Navy
Washington 25, D. C.
Attn: Code 446 (1)
463 (1)
466 (1)

1 Commanding Officer
Office of Naval Research Branch Office
346 Broadway
New York 13, New York

1 Commanding Officer
Office of Naval Research Branch Office
John Crerar Library Building
86 East Randolph Street
Chicago 1, Illinois

1 Commanding Officer
Office of Naval Research Branch Office
1030 East Green Street
Pasadena 1, California

1 Commanding Officer
Office of Naval Research Branch Office
1000 Geary Street
San Francisco 9, California

3 Commanding Officer
Office of Naval Research Branch Office
Navy #100, Fleet Post Office
New York, New York

2 Office of Naval Research
Geophysics Branch
Washington 25, D. C.
Attn: 416

1 Office of Naval Research
Resident Representative
University of Washington
Seattle 5, Washington

2 Chief, Bureau of Aeronautics
Department of the Navy
Washington 25, D. C.
Attn: PH 41 (1)
AY -3 (1)

3 Chief, Bureau of Ships
Department of the Navy
Washington 25, D. C.
Attn: Code 312 (1)
320 (1)
845 (1)

1 Chief, Bureau of Yards and Docks
Department of the Navy
Washington 25, D. C.

1 Chief of Naval Operations
Department of the Navy
Washington 25, D. C.
Attn: Op-533D

1 Commander
Naval Ordnance Laboratory, White Oak
Silver Spring 19, Maryland

1 Commanding Officer
U.S. Navy Mine Countermeasure Station
Panama City, Florida

1 Commanding Officer
U.S. Navy Underwater Sound Laboratory
New London, Connecticut

2 Department of Aerology
U.S. Naval Post Graduate School
Monterey, California

3 Director
U.S. Navy Electronics Laboratory
San Diego 52, California
Attn: 2230

6 Director
Naval Research Laboratory
Washington 25, D. C.
Attn: Technical Services Information
Officer

8 Hydrographer
U.S. Navy Hydrographic Office
Washington 25, D. C.
Attn: Division of Oceanography

10/20/54 (Rev. 10/9/58)

1 Project Arowa
U.S. Naval Air Station
Building R-48
Norfolk, Virginia

1 Superintendent
U.S. Naval Academy
Annapolis, Maryland

5 Commander
Armed Services Technical Information Agency
Attn: TIPDR
Arlington Hall Station
Arlington 12, Virginia

1 Assistant Secretary of Defense for Research and Development
Pentagon Building
Washington 25, D. C.
Attn: Committee on General Sciences

1 Commander, Air Weather Service
Scott Air Force Base, Illinois

1 Chief
Armed Forces Special Weapons Project
P.O. Box 2610
Washington, D. C.

2 Chief, U.S. Weather Bureau
2400 M Street N.W.
Washington 25, D. C.
Attn: Dr. H. Wexler

1 Commandant (OAO)
U.S. Coast Guard
Department of the Treasury
Washington 25, D. C.

1 Commanding General
Research and Development Division
Department of the Air Force
Washington 25, D. C.

1 Commanding General
Research and Development Division
Department of the Army
Washington 25, D. C.

1 Commanding Officer
Cambridge Field Station
230 Albany Street
Cambridge 30, Massachusetts
Attn: CRHSL

1 Director
U.S. Coast & Geodetic Survey
Department of Commerce
Washington 25, D. C.

2 Director, U.S. Fish & Wildlife Service
Department of the Interior
Washington 25, D. C.
Attn: Dr. L. A. Walford

1 National Research Council
2101 Constitution Avenue
Washington 25, D. C.
Attn: Committee on Undersea Warfare

1 Office of Technical Services
Department of Commerce
Washington 25, D. C.

1 U.S. Army Beach Erosion Board
5201 Little Falls Road N.W.
Washington 16, D. C.

2 U.S. Fish & Wildlife Service
Pacific Oceanic Fishery Investigation
P.O. Box 3830
Honolulu, T. H.
Attn: Librarian (1)
T.S. Austin (1)

1 U.S. Fish & Wildlife Service
Scripps Institution of Oceanography
LaJolla, California

1 U.S. Fish & Wildlife Service
Woods Hole, Massachusetts

1 U.S. Waterways Experiment Station
Vicksburg, Mississippi

1 Allen Hancock Foundation
University of Southern California
Los Angeles 7, California

1 Bingham Oceanographic Laboratories
Yale University
New Haven, Connecticut

1 Department of Conservation
Cornell University
Ithaca, New York
Attn: Dr. J. C. Ayers

1 Department of Engineering
University of California
Berkeley, California

1 Department of Meteorology & Oceanography
College of Engineering
New York University
University Heights, New York 53, N. Y.
Attn: Dr. W. J. Pierson

1 Department of Zoology
Rutgers University
New Brunswick, New Jersey
Attn: Dr. H. K. Haskins

1 Director
Bermuda Biological Station for Research
St. George's, Bermuda, B.W.I.

1 Director, Chesapeake Bay Institute
121 Maryland Hall
Johns Hopkins University
Baltimore 18, Maryland

1 Isotope Project
Hawaii Marine Laboratory
University of Hawaii
Honolulu, 14, T. H.

1 Director
Lamont Geological Observatory
Torrey Cliff
Palisades, New York

1 Director, Marine Laboratory
University of Miami
Coral Gables, Florida

1 Director
Narragansett Marine Laboratory
Kingston, Rhode Island

1 Director
National Institute of Oceanography
Wormley, Near Godalming
Surrey, England

2 Director
Scripps Institution of Oceanography
LaJolla, California

2 Director
Woods Hole Oceanographic Institution
Woods Hole, Massachusetts

1 Dr. Wayne V. Burt
Oregon State College
Corvallis, Oregon

1 Head, Department of Oceanography
Texas A & M College
College Station, Texas

1 Hudson Laboratories
Columbia University
145 Palisades Street
Dobbs Ferry, New York

1 Institute of Oceanography
University of British Columbia
Vancouver, British Columbia, Canada

2 Project Officer
Laboratory of Oceanography
Woods Hole, Massachusetts

1 Committee on Oceanography
Division of Earth Sciences
2101 Constitution Avenue
Washington 25, D. C.